Pseudo-Calibration: Improving Predictive Uncertainty Estimation in Domain Adaptation

Dapeng Hu[1] **Jian Liang**[3] **Xinchao Wang**[4] **Chuan-Sheng Foo**[2,1] *
[1]Centre for Frontier AI Research, A*STAR, Singapore
[2]Institute for Infocomm Research, A*STAR, Singapore
[3]CRIPAC & MAIS, Institute of Automation, Chinese Academy of Sciences
[4]National University of Singapore
lhxxhb15@gmail.com, liangjian92@gmail.com,
xinchao@nus.edu.sg, foo_chuan_sheng@i2r.a-star.edu.sg

Abstract

Unsupervised domain adaptation (UDA) improves model accuracy in an unlabeled target domain using a labeled source domain. However, UDA models often lack calibrated predictive uncertainty on target data, posing risks in safety-critical applications. In this paper, we address this under-explored challenge with Pseudo-Calibration (PseudoCal), a novel post-hoc calibration framework. In contrast to prior approaches, we consider UDA calibration as a target-domain specific unsupervised problem rather than a *covariate shift* problem across domains. With a synthesized labeled pseudo-target set that captures the structure of the real target, we turn the unsupervised calibration problem into a supervised one, readily solvable with *temperature scaling*. Extensive empirical evaluation across 5 diverse UDA scenarios involving 10 UDA methods, along with unsupervised fine-tuning of foundation models such as CLIP, consistently demonstrates the superior performance of PseudoCal over alternative calibration methods. Code is available at https://github.com/LHXXHB/PseudoCal.

1 Introduction

In recent years, unsupervised domain adaptation (UDA) [1] has gained popularity for enhancing the generalization of deep learning models [2, 3] across labeled source domains to an unlabeled target domain that share similar tasks but have varying data distributions. Notable progress has been achieved in developing effective UDA methods [4–6], practical applications [7, 8], and real-world settings [9–11], with a predominant focus on improving target domain model accuracy.

However, the safety-critical issue of calibrating predictive uncertainty, extensively studied in IID scenarios [12, 13], remains largely under-explored in UDA. Figure 1(a) illustrates that increasing target domain accuracy is accompanied by significant overfitting of the negative log-likelihood (NLL) loss during adaptation. The two primary challenges in addressing predictive uncertainty calibration in UDA are the absence of labeled target data and severe distribution shifts between the two domains. Therefore, traditional supervised calibration methods like *temperature scaling* [12] are inapplicable. Recent studies [14–16] address the first challenge by employing *importance-weighting* [17] with labeled source data. However, they still suffer from the second challenge and other critical drawbacks such as additional complex density modeling and inapplicability in privacy-preserving UDA scenarios like source-free UDA settings [18, 11, 19] and unsupervised adaptation of foundation models [20].

*Corresponding author.

Workshop on Distribution Shifts, 37th Conference on Neural Information Processing Systems (NeurIPS 2023).

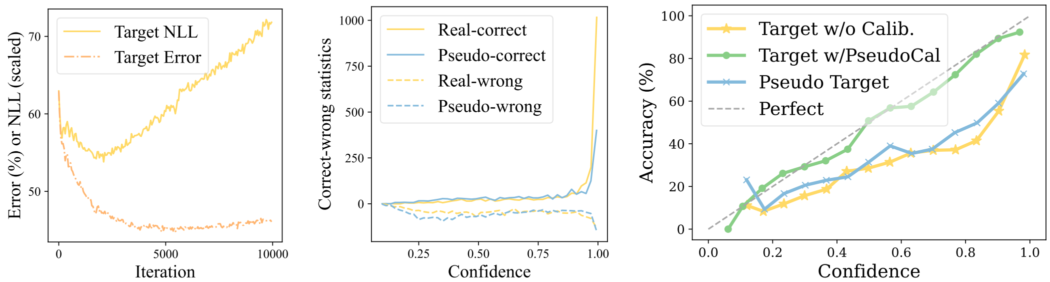

(a) Overfitting of NLL (b) Correct-wrong statistics (c) Reliability diagrams

Figure 1: ATDOC [21] on a closed-set UDA task Ar $\rightarrow$ Cl. (a) illustrates the target error and target NLL loss (rescaled to match error) during UDA training. (b) divides confidence values into 50 bins, displaying the count of correct and wrong predictions in each bin. For real target data, correctness is determined by comparing predictions with ground truths, and for pseudo-target data, it's assessed by comparing predictions with synthesized labels. (c) shows reliability diagrams [12] for both pseudo and real target data. Perfect: ideal predictions without miscalibrations.

In contrast to the covariate shift view in [14–16], we adopt a novel perspective, treating UDA calibration as an unsupervised calibration problem specific to the target domain. We first study the 'Oracle' case of using labeled target data for *temperature scaling* and then factorize its NLL objective into a joint optimization involving both correct and wrong predictions. This factorization uncovers a key insight with *temperature scaling*: datasets with similar correct-wrong statistics should share similar temperatures. Inspired by this insight, we introduce a novel post-hoc calibration framework called Pseudo-Calibration (PseudoCal). PseudoCal is based on *temperature scaling* and estimates the temperature for target data through calibration on a synthesized labeled pseudo-target dataset that mimics similar correct-wrong statistics as the real target data. Concretely, PseudoCal utilizes *mixup* [22] during the inference stage with unlabeled target data to generate a labeled pseudo-target set. It then performs supervised calibration on this labeled set to determine the final temperature. PseudoCal's effectiveness depends on the presence of similar correct-wrong statistics between pseudo and real target data. We elucidate the behind support with an intuitive analysis grounded in the well-established *cluster assumption* [23]. Specifically, pseudo-target samples with correct predictions correspond to correct real target samples, and vice versa, as shown in Figure 1(b). Benefitting from the high resemblance of correct-wrong statistics between our synthesized pseudo-target and real target, PseudoCal achieves significantly improved calibration performance, as demonstrated in Figure 1(c).

2 Approach

We introduce UDA with a C-way image classification task. UDA generally involves a labeled source domain and an unlabeled target domain. The source domain $\mathcal{D}_\text{s} = \{(x_\text{s}^i, y_\text{s}^i)\}_{i=1}^{n_\text{s}}$ consists of n_s images x_s with labels y_s, where $x_\text{s}^i \in \mathcal{X}_\text{s}$ and $y_\text{s}^i \in \mathcal{Y}_\text{s}$. The target domain $\mathcal{D}_\text{t} = \{x_\text{t}^i\}_{i=1}^{n_\text{t}}$ contains unlabeled images x_t, where $x_\text{t}^i \in \mathcal{X}_\text{t}$. UDA aims to learn a model ϕ that can predict the unknown labels $\{y_\text{t}^i\}_{i=1}^{n_\text{t}}$ for the target domain, utilizing data from both domains simultaneously [4] or sequentially [11]. Given a sample (x, y) and UDA model ϕ, we can obtain the predicted class $\hat{y}$ and its softmax-based confidence $\hat{p}$. Ideally, $\hat{p}$ should accurately reflect the probability of correctness, expressed as $\mathbb{P}(\hat{y} = y|\hat{p} = p) = p,\ \forall\, p \in [0, 1]$. This perfect calibration, also known as *Perfect*, is impossible to achieve [12]. A widely used metric for evaluating calibration error is the expected calibration error (ECE) [12]. Kindly refer to Appendix C for details of ECE and other metrics.

2.1 Supervised 'Oracle': Factorized Temperature Scaling

Temperature scaling (TempScal) [12] is a post-hoc calibration method that optimizes a temperature scalar, denoted as T, on a labeled validation set with the NLL loss. In UDA, we define the calibration achieved by applying TempScal with target raw predictions and unattainable target ground truths as the 'Oracle' calibration and the corresponding temperature as T_o. Let z represent the logit vector for input x, and let $\sigma(\cdot)$ denote softmax. Kindly refer to Appendix C for details of TempScal. We propose the following novel factorization of the NLL objective:

$$T_\text{o} = \arg\min_T \frac{N_\text{c}}{N}\mathbb{E}_{(x_\text{t}^i, y_\text{t}^i)\in\mathcal{D}_\text{c}}\, \mathcal{L}_\text{NLL}\left(\sigma(z_\text{t}^i/T), y_\text{t}^i\right) + \frac{N_\text{w}}{N}\mathbb{E}_{(x_\text{t}^j, y_\text{t}^j)\in\mathcal{D}_\text{w}}\, \mathcal{L}_\text{NLL}\left(\sigma(z_\text{t}^j/T), y_\text{t}^j\right), \quad (1)$$

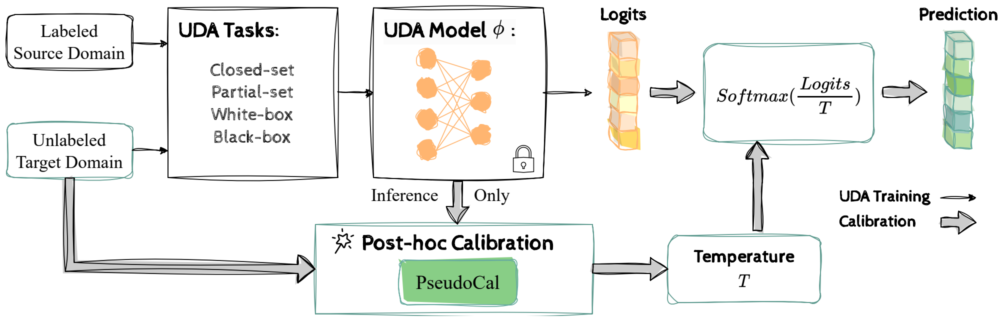

Figure 2: The pipeline of PseudoCal for calibrating predictive uncertainty in UDA.

where $\mathcal{D}_{\mathrm{c}}$ represents the dataset of correctly predicted samples, comprising N_{c} instances. Similarly, $\mathcal{D}_{\mathrm{w}}$ denotes the dataset of wrongly predicted samples, consisting of N_{w} instances. Both types of samples have contrasting effects on the temperature optimization process. NLL minimization favors a small temperature to sharpen the correct predictions and a large temperature to flatten the wrong predictions. This implies that datasets with similar correct-wrong statistics are likely to obtain similar temperatures when using TempScal for supervised calibration.

2.2 Unsupervised Solution: Pseudo-Calibration

Inspired by this factorization, we introduce our Pseudo-Calibration (PseudoCal) framework. The main idea is to use the unlabeled target data to synthesize a labeled pseudo-target set that mimics the correct-wrong statistics of the real target set and then apply TempScal to this labeled set. In PseudoCal, we employ *mixup* [22] with data across clusters (i.e., with different pseudo-labels), generating mixed samples that inherently include both correct and wrong predictions when evaluated with mixed labels. Moreover, we can expect sample-level correspondences between mixed and real samples according to *cluster assumption* [23]. Kindly refer to Appendix D for further analysis. Specifically, PseudoCal consists of the following two simple steps. The pipeline of PseudoCal is illustrated in Figure 2, where the UDA model is utilized as a black box solely for inferring the predictions of input data. A comprehensive Pytorch-style pseudocode for PseudoCal is provided in Appendix A.

Step 1: Pseudo-target synthesis. We generate a pseudo-target set by applying *mixup* to target samples in the inference stage. Specifically, a pseudo-target sample x_{pt} and its label y_{pt} are obtained by taking a convex combination of a pair of real target samples $x_{\mathrm{t}}^i, x_{\mathrm{t}}^j$ from different clusters and their pseudo-labels $\hat{y}_{\mathrm{t}}^i, \hat{y}_{\mathrm{t}}^j$. Consequently, we obtain a labeled pseudo-target set $\{(x_{\mathrm{pt}}^i, y_{\mathrm{pt}}^i)\}_{i=1}^{n_{\mathrm{pt}}}$, where n_{pt} represents the amount. The general process of pseudo-target synthesis is formulated as $x_{\mathrm{pt}} = \lambda * x_{\mathrm{t}}^i + (1-\lambda) * x_{\mathrm{t}}^j, y_{\mathrm{pt}} = \lambda * \hat{y}_{\mathrm{t}}^i + (1-\lambda) * \hat{y}_{\mathrm{t}}^j$, where $\lambda \in (0.5, 1.0)$ is the mix ratio.

Step 2: Supervised calibration. Using the synthesized labeled pseudo-target set $\{(x_{\mathrm{pt}}^i, y_{\mathrm{pt}}^i)\}_{i=1}^{n_{\mathrm{pt}}}$, we can easily determine the optimal pseudo-target temperature through TempScal. This estimated temperature serves as an approximation of the 'Oracle' target temperature T_{o}.

3 Experiments

Datasets. For classification, we adopt 5 popular UDA benchmarks, including *Office-31* [24], *Office-Home* [25], *VisDA* [26], *DomainNet* [27], and *Image-Sketch* [28]. For semantic segmentation, we use synthetic-to-real benchmarks with *Cityscapes*[29], *GTA5*[30], and *SYNTHIA* [31].

Methods. For calibration methods, we consider 5 typical calibration baselines in UDA, including the no calibration baseline (No Calib.), source-domain calibration (TempScal-src [12]), cross-domain calibration (CPCS [14], TransCal [16]), and generic calibration (Ensemble [13]). We evaluate model calibration on 10 UDA methods across 5 UDA scenarios. For image classification, we cover closed-set UDA methods (ATDOC [21], BNM [32], MCC [33], CDAN [5], SAFN [34], MCD [6]), partial-set UDA methods (ATDOC [21], MCC [33], PADA [10]), the whit-box source-free UDA method (SHOT [11]), the black-box source-free UDA method (DINE [19]), and unsupervised adaptation of CLIP [35] by POUF [20]. For semantic segmentation, we focus on calibrating source-only models without any adaptation. Kindly refer to Appendix B for more information on these baselines. PseudoCal uses a fixed mixing ratio of $\lambda = 0.65$ for all results, except for POUF, where it's 0.8.

Results of data-dependent UDA. Results are averaged over five random runs and across UDA tasks sharing the same target domain. Table 1 shows results of closed-set UDA on *DomainNet*. PseudoCal consistently achieves a low ECE close to 'Oracle', surpassing the second-best calibration method CPCS by 5.95% on average on this large-scale UDA benchmark.

Results of source-free UDA. We assess source-free UDA with SHOT and DINE. In the scenario using foundation models, we employ POUF. Specifically, POUF fine-tunes the CLIP model as a source model with unlabeled target data. Table 2 presents source-free UDA results, and Table 3 shows POUF results. PseudoCal significantly outperforms Ensemble in source-free UDA, with a margin of 7.44% on *DomainNet* and 15.05% on *Image-Sketch*. In CLIP experiments, PseudoCal also demonstrates effective ECE error reduction across all unsupervised fine-tuning tasks.

In Appendix E, we have provided comprehensive results and analysis of PseudoCal.

Table 1: ECE (%) of closed-set UDA on *DomainNet* (*DNet*). **bold**: Best value.

Method	ATDOC [21]					BNM [32]					MCC [33]				
	→C	→P	→R	→S	avg	→C	→P	→R	→S	avg	→C	→P	→R	→S	avg
No Calib.	9.54	7.38	3.75	12.29	8.24	28.57	22.10	15.37	31.27	24.33	8.63	7.77	4.79	13.61	8.70
TempScal [12]	8.69	7.71	1.94	11.82	7.54	19.04	13.62	9.40	20.30	15.59	8.38	8.32	**2.36**	13.88	8.23
CPCS [14]	10.78	4.72	4.46	13.38	8.34	8.23	7.92	7.98	9.29	8.36	9.03	4.33	3.44	17.21	8.50
TransCal [16]	23.02	24.76	26.65	19.68	23.52	**6.52**	**1.84**	**5.82**	9.39	**5.89**	22.27	24.06	23.45	18.03	21.95
Ensemble [13]	6.32	4.54	**1.59**	9.05	5.37	23.44	18.61	12.61	26.21	20.22	5.71	5.10	2.57	10.34	5.93
PseudoCal	**1.82**	**1.41**	2.51	**1.70**	**1.86**	10.27	6.01	6.18	**5.86**	7.08	**1.35**	**1.89**	2.38	**3.10**	**2.18**
Oracle	1.55	0.94	0.86	1.07	1.10	2.40	1.66	3.40	1.30	2.19	1.16	1.44	1.09	0.89	1.14
Accuracy (%)	56.05	60.64	74.95	52.08	60.93	56.62	63.13	74.30	52.25	61.57	50.89	57.74	71.62	46.39	56.66

Method	CDAN [5]					SAFN [34]					MCD [6]					*DNet*
	→C	→P	→R	→S	avg	→C	→P	→R	→S	avg	→C	→P	→R	→S	avg	AVG
No Calib.	10.17	9.64	5.56	14.44	9.95	17.94	14.44	10.15	21.26	15.95	9.56	7.40	3.80	12.93	8.42	12.60
TempScal [12]	7.92	8.31	2.75	12.30	7.82	9.61	8.15	4.12	14.18	9.02	6.48	6.96	4.06	11.20	7.18	9.23
CPCS [14]	10.75	4.28	5.57	6.91	6.88	10.92	5.91	8.22	22.59	11.91	7.02	3.51	1.96	21.79	8.57	8.76
TransCal [16]	20.92	21.41	22.93	16.93	20.55	10.75	12.88	14.28	6.88	11.20	21.48	24.99	27.45	18.95	23.22	17.72
Ensemble [13]	7.21	6.74	3.54	11.29	7.20	16.59	13.25	9.08	19.52	14.61	7.25	5.27	2.86	11.34	6.68	10.00
PseudoCal	**1.58**	**1.89**	**1.86**	**2.67**	**2.00**	**3.33**	**1.30**	**1.50**	**2.76**	**2.22**	**2.27**	**1.16**	**1.01**	**1.70**	**1.53**	**2.81**
Oracle	1.45	1.08	1.07	0.94	1.13	1.43	0.92	1.21	0.72	1.07	1.33	0.97	0.56	0.68	0.88	1.25
Accuracy (%)	53.11	59.13	71.82	49.09	58.29	49.59	58.03	66.40	47.66	55.42	48.85	57.99	65.32	47.95	55.03	57.98

Table 2: ECE (%) of source-free UDA on *DomainNet* (*DNet*) and *ImageNet-Sketch* (*Sketch*).

Method	SHOT [11]						DINE [19]						*DNet*	*Sketch*
	→C	→P	→R	→S	avg	I→S	→C	→P	→R	→S	avg	I→S	AVG	AVG
No Calib.	17.16	21.19	10.03	23.14	17.88	34.71	21.99	22.51	12.39	30.34	21.81	58.85	19.84	46.78
Ensemble [13]	14.24	17.94	7.81	19.49	14.87	33.03	17.88	18.86	10.83	25.33	18.22	53.24	16.54	43.14
PseudoCal	**6.66**	**7.78**	**2.91**	**6.67**	**6.00**	**8.42**	**14.42**	**12.95**	**5.30**	**16.15**	**12.20**	**47.76**	**9.10**	**28.09**
Oracle	3.27	2.52	1.37	2.18	2.33	4.39	1.75	1.80	1.29	1.37	1.55	5.90	1.94	5.14
Accuracy (%)	66.52	64.48	78.34	59.64	67.25	34.29	63.76	65.47	80.69	55.51	66.36	22.27	66.80	28.28

Table 3: ECE (%) of the fine-tuned CLIP model using POUF [20] with unlabeled target-domain data.

Method	*Office*			*Office-Home*				*VisDA*		*DomainNet*			
	A	W	D	Ar	Cl	Pr	Re	T	V	C	P	R	S
No Calib.	7.86	6.22	3.08	10.81	20.07	9.06	11.14	8.57	6.52	4.10	4.89	2.06	6.32
PseudoCal	**2.37**	**4.52**	**2.29**	**7.95**	**4.73**	**6.60**	**7.85**	**2.71**	**1.97**	**3.74**	**3.80**	**1.88**	**1.38**
Oracle	2.04	3.11	1.20	5.70	3.87	6.11	6.72	2.50	0.39	1.51	1.00	1.13	0.97
Accuracy (%)	84.03	84.54	86.42	77.63	61.81	83.98	80.54	86.37	86.72	81.75	82.01	89.96	79.08

4 Conclusion

In conclusion, we introduce PseudoCal, a novel and versatile post-hoc framework for calibrating predictive uncertainty in unsupervised domain adaptation (UDA). By focusing on the unlabeled target domain, PseudoCal distinguishes itself from mainstream calibration methods that are based on *covariate shift* and eliminates their associated limitations. To elaborate, PseudoCal employs a novel inference-stage *mixup* strategy to synthesize a labeled pseudo-target set that mimics the correct-wrong statistics in real target samples. In this way, PseudoCal successfully transforms the challenging unsupervised calibration problem involving unlabeled real samples into a supervised one using labeled pseudo-target data, which can be readily addressed through *temperature scaling*. Throughout our extensive evaluations spanning diverse UDA settings beyond *covariate shift*, including source-free UDA settings and domain adaptive semantic segmentation, PseudoCal consistently showcases its advantages of simplicity, versatility, and effectiveness in enhancing calibration in UDA.

References

[1] Pan, S. J., Q. Yang. A survey on transfer learning. *IEEE Transactions on Knowledge and Data Engineering*, 22(10):1345–1359, 2009.

[2] He, K., X. Zhang, S. Ren, et al. Deep residual learning for image recognition. In *IEEE Conference on Computer Vision and Pattern Recognition*. 2016.

[3] Dosovitskiy, A., L. Beyer, A. Kolesnikov, et al. An image is worth 16x16 words: Transformers for image recognition at scale. In *International Conference on Learning Representations*. 2021.

[4] Ganin, Y., V. Lempitsky. Unsupervised domain adaptation by backpropagation. In *International Conference on Machine Learning*. 2015.

[5] Long, M., Z. Cao, J. Wang, et al. Conditional adversarial domain adaptation. In *Advances in Neural Information Processing Systems*. 2018.

[6] Saito, K., K. Watanabe, Y. Ushiku, et al. Maximum classifier discrepancy for unsupervised domain adaptation. In *IEEE Conference on Computer Vision and Pattern Recognition*. 2018.

[7] Chen, Y., W. Li, C. Sakaridis, et al. Domain adaptive faster r-cnn for object detection in the wild. In *IEEE Conference on Computer Vision and Pattern Recognition*. 2018.

[8] Tsai, Y.-H., W.-C. Hung, S. Schulter, et al. Learning to adapt structured output space for semantic segmentation. In *IEEE Conference on Computer Vision and Pattern Recognition*. 2018.

[9] Long, M., Y. Cao, J. Wang, et al. Learning transferable features with deep adaptation networks. In *International Conference on Machine Learning*. 2015.

[10] Cao, Z., L. Ma, M. Long, et al. Partial adversarial domain adaptation. In *European Conference on Computer Vision*. 2018.

[11] Liang, J., D. Hu, J. Feng. Do we really need to access the source data? source hypothesis transfer for unsupervised domain adaptation. In *International Conference on Machine Learning*. 2020.

[12] Guo, C., G. Pleiss, Y. Sun, et al. On calibration of modern neural networks. In *International Conference on Machine Learning*. 2017.

[13] Lakshminarayanan, B., A. Pritzel, C. Blundell. Simple and scalable predictive uncertainty estimation using deep ensembles. In *Advances in Neural Information Processing Systems*. 2017.

[14] Park, S., O. Bastani, J. Weimer, et al. Calibrated prediction with covariate shift via unsupervised domain adaptation. In *International Conference on Artificial Intelligence and Statistics*. 2020.

[15] Pampari, A., S. Ermon. Unsupervised calibration under covariate shift. *arXiv preprint arXiv:2006.16405*, 2020.

[16] Wang, X., M. Long, J. Wang, et al. Transferable calibration with lower bias and variance in domain adaptation. In *Advances in Neural Information Processing Systems*. 2020.

[17] Cortes, C., M. Mohri, M. Riley, et al. Sample selection bias correction theory. In *Algorithmic Learning Theory*. 2008.

[18] Li, R., Q. Jiao, W. Cao, et al. Model adaptation: Unsupervised domain adaptation without source data. In *IEEE Conference on Computer Vision and Pattern Recognition*. 2020.

[19] Liang, J., D. Hu, J. Feng, et al. Dine: Domain adaptation from single and multiple black-box predictors. In *IEEE Conference on Computer Vision and Pattern Recognition*. 2022.

[20] Tanwisuth, K., S. Zhang, H. Zheng, et al. Pouf: Prompt-oriented unsupervised fine-tuning for large pre-trained models. In *International Conference on Machine Learning*. 2023.

[21] Liang, J., D. Hu, J. Feng. Domain adaptation with auxiliary target domain-oriented classifier. In *IEEE Conference on Computer Vision and Pattern Recognition*. 2021.

[22] Zhang, H., M. Cisse, Y. N. Dauphin, et al. mixup: Beyond empirical risk minimization. In *International Conference on Learning Representations*. 2018.

[23] Grandvalet, Y., Y. Bengio. Semi-supervised learning by entropy minimization. In *Advances in Neural Information Processing Systems*. 2004.

[24] Saenko, K., B. Kulis, M. Fritz, et al. Adapting visual category models to new domains. In *European Conference on Computer Vision*. 2010.

[25] Venkateswara, H., J. Eusebio, S. Chakraborty, et al. Deep hashing network for unsupervised domain adaptation. In *IEEE Conference on Computer Vision and Pattern Recognition*. 2017.

[26] Peng, X., B. Usman, N. Kaushik, et al. Visda: The visual domain adaptation challenge. *arXiv preprint arXiv:1710.06924*, 2017.

[27] Peng, X., Q. Bai, X. Xia, et al. Moment matching for multi-source domain adaptation. In *IEEE International Conference on Computer Vision*. 2019.

[28] Wang, H., S. Ge, Z. Lipton, et al. Learning robust global representations by penalizing local predictive power. In *Advances in Neural Information Processing Systems*. 2019.

[29] Cordts, M., M. Omran, S. Ramos, et al. The cityscapes dataset for semantic urban scene understanding. In *IEEE Conference on Computer Vision and Pattern Recognition*. 2016.

[30] Richter, S. R., V. Vineet, S. Roth, et al. Playing for data: Ground truth from computer games. In *European Conference on Computer Vision*. 2016.

[31] Ros, G., L. Sellart, J. Materzynska, et al. The synthia dataset: A large collection of synthetic images for semantic segmentation of urban scenes. In *IEEE Conference on Computer Vision and Pattern Recognition*. 2016.

[32] Cui, S., S. Wang, J. Zhuo, et al. Towards discriminability and diversity: Batch nuclear-norm maximization under label insufficient situations. In *IEEE Conference on Computer Vision and Pattern Recognition*. 2020.

[33] Jin, Y., X. Wang, M. Long, et al. Minimum class confusion for versatile domain adaptation. In *European Conference on Computer Vision*. 2020.

[34] Xu, R., G. Li, J. Yang, et al. Larger norm more transferable: An adaptive feature norm approach for unsupervised domain adaptation. In *IEEE International Conference on Computer Vision*. 2019.

[35] Radford, A., J. W. Kim, C. Hallacy, et al. Learning transferable visual models from natural language supervision. In *International Conference on Machine Learning*. 2021.

[36] Gal, Y., Z. Ghahramani. Dropout as a bayesian approximation: Representing model uncertainty in deep learning. In *International Conference on Machine Learning*. 2016.

[37] Sun, B., K. Saenko. Deep coral: Correlation alignment for deep domain adaptation. In *European Conference on Computer Vision, Workshop*. 2016.

[38] Tzeng, E., J. Hoffman, K. Saenko, et al. Adversarial discriminative domain adaptation. In *IEEE Conference on Computer Vision and Pattern Recognition*. 2017.

[39] Shu, R., H. H. Bui, H. Narui, et al. A dirt-t approach to unsupervised domain adaptation. *arXiv preprint arXiv:1802.08735*, 2018.

[40] Vu, T.-H., H. Jain, M. Bucher, et al. Advent: Adversarial entropy minimization for domain adaptation in semantic segmentation. In *IEEE Conference on Computer Vision and Pattern Recognition*. 2019.

[41] Sugiyama, M., M. Krauledat, K.-R. Müller. Covariate shift adaptation by importance weighted cross validation. *Journal of Machine Learning Research*, 8(5), 2007.

[42] Lipton, Z., Y.-X. Wang, A. Smola. Detecting and correcting for label shift with black box predictors. In *International Conference on Machine Learning*. 2018.

[43] Liang, J., Y. Wang, D. Hu, et al. A balanced and uncertainty-aware approach for partial domain adaptation. In *European Conference on Computer Vision*. 2020.

[44] Panareda Busto, P., J. Gall. Open set domain adaptation. In *IEEE International Conference on Computer Vision*. 2017.

[45] Zhang, H., Y. Zhang, K. Jia, et al. Unsupervised domain adaptation of black-box source models. *arXiv preprint arXiv:2101.02839*, 2021.

[46] Zadrozny, B., C. Elkan. Obtaining calibrated probability estimates from decision trees and naive bayesian classifiers. In *International Conference on Machine Learning*. 2001.

[47] —. Transforming classifier scores into accurate multiclass probability estimates. In *ACM SIGKDD International Conference on Knowledge Discovery and Data Mining*. 2002.

[48] Platt, J., et al. Probabilistic outputs for support vector machines and comparisons to regularized likelihood methods. *Advances in Large Margin Classifiers*, 10(3):61–74, 1999.

[49] Blundell, C., J. Cornebise, K. Kavukcuoglu, et al. Weight uncertainty in neural network. In *International Conference on Machine Learning*. 2015.

[50] Louizos, C., M. Welling. Multiplicative normalizing flows for variational bayesian neural networks. In *International Conference on Machine Learning*. 2017.

[51] Wen, Y., P. Vicol, J. Ba, et al. Flipout: Efficient pseudo-independent weight perturbations on mini-batches. *arXiv preprint arXiv:1803.04386*, 2018.

[52] Ovadia, Y., E. Fertig, J. Ren, et al. Can you trust your model's uncertainty? evaluating predictive uncertainty under dataset shift. In *Advances in Neural Information Processing Systems*. 2019.

[53] Alexandari, A., A. Kundaje, A. Shrikumar. Maximum likelihood with bias-corrected calibration is hard-to-beat at label shift adaptation. In *International Conference on Machine Learning*. 2020.

[54] Ding, Z., X. Han, P. Liu, et al. Local temperature scaling for probability calibration. In *IEEE International Conference on Computer Vision*. 2021.

[55] Wang, D., B. Gong, L. Wang. On calibrating semantic segmentation models: Analysis and an algorithm. *arXiv preprint arXiv:2212.12053*, 2022.

[56] de Jorge, P., R. Volpi, P. Torr, et al. Reliability in semantic segmentation: Are we on the right track? *arXiv preprint arXiv:2303.11298*, 2023.

[57] Tomani, C., S. Gruber, M. E. Erdem, et al. Post-hoc uncertainty calibration for domain drift scenarios. In *IEEE Conference on Computer Vision and Pattern Recognition*. 2021.

[58] Salvador, T., V. Voleti, A. Iannantuono, et al. Improved predictive uncertainty using corruption-based calibration. *STAT*, 1050:7, 2021.

[59] Tomani, C., F. K. Waseda, Y. Shen, et al. Beyond in-domain scenarios: Robust density-aware calibration. In *International Conference on Machine Learning*. 2023.

[60] Gong, Y., X. Lin, Y. Yao, et al. Confidence calibration for domain generalization under covariate shift. In *IEEE International Conference on Computer Vision*. 2021.

[61] Yu, Y., S. Bates, Y. Ma, et al. Robust calibration with multi-domain temperature scaling. In *Advances in Neural Information Processing Systems*. 2022.

[62] Thulasidasan, S., G. Chennupati, J. A. Bilmes, et al. On mixup training: Improved calibration and predictive uncertainty for deep neural networks. In *Advances in Neural Information Processing Systems*. 2019.

[63] Liu, B., I. Ben Ayed, A. Galdran, et al. The devil is in the margin: Margin-based label smoothing for network calibration. In *IEEE Conference on Computer Vision and Pattern Recognition*. 2022.

[64] Krishnan, R., O. Tickoo. Improving model calibration with accuracy versus uncertainty optimization. In *Advances in Neural Information Processing Systems*. 2020.

[65] Goodfellow, I., Y. Bengio, A. Courville. *Deep learning*. MIT press, 2016.

[66] Brier, G. W., et al. Verification of forecasts expressed in terms of probability. *Monthly Weather Review*, 78(1):1–3, 1950.

[67] Chapelle, O., A. Zien. Semi-supervised classification by low density separation. In *International Workshop on Artificial Intelligence and Statistics*. 2005.

[68] Verma, V., K. Kawaguchi, A. Lamb, et al. Interpolation consistency training for semi-supervised learning. *Neural Networks*, 145:90–106, 2022.

[69] Fu, B., Z. Cao, M. Long, et al. Learning to detect open classes for universal domain adaptation. In *European Conference on Computer Vision*. 2020.

[70] Bucci, S., M. R. Loghmani, T. Tommasi. On the effectiveness of image rotation for open set domain adaptation. In *European Conference on Computer Vision*. 2020.

[71] Saito, K., D. Kim, S. Sclaroff, et al. Semi-supervised domain adaptation via minimax entropy. In *IEEE International Conference on Computer Vision*. 2019.

[72] Guo, H., Y. Mao, R. Zhang. Mixup as locally linear out-of-manifold regularization. In *AAAI Conference on Artificial Intelligence*. 2019.

[73] Müller, R., S. Kornblith, G. E. Hinton. When does label smoothing help? In *Advances in Neural Information Processing Systems*. 2019.

[74] Chen, X., H. Fan, R. Girshick, et al. Improved baselines with momentum contrastive learning. *arXiv preprint arXiv:2003.04297*, 2020.

[75] Cubuk, E. D., B. Zoph, J. Shlens, et al. Randaugment: Practical automated data augmentation with a reduced search space. In *IEEE Conference on Computer Vision and Pattern Recognition, Workshops*. 2020.

[76] Yun, S., D. Han, S. J. Oh, et al. Cutmix: Regularization strategy to train strong classifiers with localizable features. In *IEEE International Conference on Computer Vision*. 2019.

[77] Verma, V., A. Lamb, C. Beckham, et al. Manifold mixup: Better representations by interpolating hidden states. In *International Conference on Machine Learning*. 2019.

[78] Lee, D.-H., et al. Pseudo-label: The simple and efficient semi-supervised learning method for deep neural networks. In *International Conference on Machine Learning, Workshop*. 2013.

[79] Sohn, K., D. Berthelot, N. Carlini, et al. Fixmatch: Simplifying semi-supervised learning with consistency and confidence. In *Advances in Neural Information Processing Systems*. 2020.

A Algorithm

The PyTorch-style pseudocode for our calibration method PseudoCal is provided in Algorithm 1.

Algorithm 1 PyTorch-style pseudocode for PseudoCal.

```
# x: A batch of real target images with shuffled order.
# lam: The mix ratio, a fixed scalar value between 0.5 and 1.0.
# net: A trained UDA model in the evaluation mode.

# Perform pseudo-target synthesis for a mini-batch.
def pseudo_target_synthesis(x, lam, net):

    # Use the random index within the data batch
    # to obtain a pair of real samples for mixup.
    rand_idx = torch.randperm(x.shape[0])
    inputs_a = x
    inputs_b = x[rand_idx]

    # Obtain model predictions and pseudo labels (pl).
    pred_a = net(inputs_a)
    pl_a = pred_a.max(dim=1)[1]
    pl_b = pl_a[rand_idx]

    # Select the samples with distinct labels for the mixup.
    diff_idx = (pl_a != pl_b).nonzero(as_tuple=True)[0]

    # Mixup with images and labels.
    pseudo_target_x = lam * inputs_a + (1 - lam) * inputs_b

    # If the user is not aware that lam is between 0.5 and 1.0,
    # the following if-else code can avoid bugs.
    if lam > 0.5:
        pseudo_target_y = pl_a
    else:
        pseudo_target_y = pl_b

    return pseudo_target_x[diff_idx], pseudo_target_y[diff_idx]

# Perform supervised calibration using pseudo-target data.
def pseudoCal(x, lam, net):

    # Synthesize a mini-batch of pseudo-target samples and labels.
    pseudo_x, pseudo_y = pseudo_target_synthesis(x, lam, net)

    # Infer the logits for the pseudo-target samples.
    pseudo_logit = net(pseudo_x)

    # Apply temperature scaling to estimate the
    # pseudo-target temperature as the real temperature.
    calib_method = TempScaling()
    pseudo_temp = calib_method(pseudo_logit, pseudo_y)

    return pseudo_temp
```

B Related Work

Unsupervised domain adaptation (UDA) has been extensively studied in image classification tasks. Mainstream methods can be categorized into two lines: 1) Distribution alignment across domains using specific discrepancy measures [9, 37] or adversarial learning [4, 38, 5, 6], and 2) Target domain-based learning with self-training [39, 21] or regularizations [34, 32, 33]. Moreover, UDA has also

Table 4: Comparisons of typical methods for predictive uncertainty calibration in UDA.

Calibration Method	Covariate Shift	Label Shift	No harm to accuracy	No extra training	No source data
TempScal-src [12]	✗	✗	✓	✓	✗
MC-Dropout [36]	✓	✓	✗	✓	✓
Ensemble [13]	✓	✓	✓	✗	✓
CPCS [14]	✓	✗	✓	✗	✗
TransCal [16]	✓	✗	✓	✗	✗
PseudoCal (Ours)	✓	✓	✓	✓	✓

been studied in object detection [7, 6] and image segmentation [8, 40]. Initially, UDA was based on the *covariate shift* assumption [41] – two domains share similar label and conditional distributions but have different input distributions. This is commonly referred to as closed-set UDA. In recent years, new practical settings have arisen, notably addressing label shift [42]. These include partial-set UDA [10, 43], where some source classes are absent in the target domain, and open-set UDA [44], where the target domain includes samples from unknown classes. Recently, there has been a growing interest in a setting called source-free UDA, which can preserve source privacy. Source-free UDA has two key settings: the white-box setting [18, 11] uses the source model for target adaptation, while the stricter black-box setting [45, 19] only employs the source model for inference.

Predictive uncertainty calibration was initially stuidied on binary classification tasks [46–48]. [12] extends *Platt scaling* [48] to multi-class classification and introduces *matrix scaling* (MatrixScal), *vector scaling* (VectorScal), and *temperature scaling* (TempScal). These post-hoc methods require a labeled validation set for calibration. On the other hand, there are methods that address calibration during model training, including *Monte Carlo Dropout* (MC-Dropout) [36], Ensemble [13], and *Stochastic Variational Bayesian Inference* (SVI) [49–51]. However, an evaluation in [52] reveals that these methods do not maintain calibration performance under dataset shift. In addition, there is growing interest in calibration under distribution shifts [53, 16, 14] and in semantic segmentation tasks [54–56]. In this paper, we specifically address the calibration problem in single-source UDA. A vanilla baseline is to apply IID calibration methods such as TempScal with a labeled source validation set, dubbed TempScal-src. Regarding calibration methods considering the domain distribution shifts, the mainstream idea is to utilize *importance weighting* [17] to address calibration under *covariate shift* in UDA, exemplified by CPCS [14] and TransCal [16]. Some works perturb the source validation set to serve as a general target set [57, 58] or employ it for density estimation [59]. More recently, some methods [60, 61] have utilized multiple source domains to calibrate the unlabeled target domain in UDA. Additionally, there are training-stage calibration methods that employ smoothed labels [62, 63] or optimize accuracy-uncertainty differentiably [64]. Among these methods, CPCS and TransCal are noteworthy as they specifically address transductive target calibration in UDA. For more general approaches like MC-Dropout and Ensemble, we compare our method directly with Ensemble because it consistently outperforms MC-Dropout. Table 4 presents a comprehensive comparison of these typical UDA calibration methods. In contrast to existing calibration methods, PseudoCal stands out by not requiring any extra model training. It is a simple, post-hoc, and general calibration approach, solely relying on a fixed or even black-box UDA model and unlabeled target data for calibration.

C Calibration Metrics

Optimization of *temperature scaling* [12]. The 'Oracle' target temperature, denoted as T_o, can be obtained using the original *temperature scaling* optimization formulated as follows.

$$T_\mathrm{o} = \arg\min_{T} \mathbb{E}_{(x_\mathrm{t}^i, y_\mathrm{t}^i)\in\mathcal{D}_\mathrm{t}} \mathcal{L}_\mathrm{NLL}\left(\sigma(z_\mathrm{t}^i/T), y_\mathrm{t}^i\right)$$

Let $\mathbf{y}_i$ represent the one-hot ground truth encoding for input sample x_i, and $\hat{\mathbf{p}}_i$ denote the predicted probability vector output by the model ϕ.

Expected Calibration Error (ECE) [12] involves partitioning probability predictions into M bins, with B_m representing the indices of samples falling into the m-th bin. It calculates the weighted average of the accuracy-confidence difference across all bins:

$$\mathcal{L}_{\mathrm{ECE}} = \sum_{m=1}^{M} \frac{|B_m|}{n} |\mathrm{acc(B_m)} - \mathrm{conf(B_m)}|$$

Here, n represents the number of samples, and for the m-th bin, the accuracy is computed as $\mathrm{acc}\ (B_m) = |B_m|^{-1} \sum_{i \in B_m} \mathbb{1}(\hat{y}_i = y_i)$, and the confidence is computed as $\mathrm{conf}\ (B_m) = |B_m|^{-1} \sum_{i \in B_m} \hat{p}_i$.

Negative Log-Likelihood (NLL) [65] is also known as the cross-entropy loss. The NLL loss for a single sample x_i is given by:

$$\mathcal{L}_{\mathrm{NLL}} = -\sum_{c=1}^{C} \mathbf{y}_i^c \log \hat{\mathbf{p}}_i^c$$

Brier Score (BS) [66] can be defined as the squared error between the predicted probability vector and the one-hot label vector. The Brier Score for a single sample x_i is given by:

$$\mathcal{L}_{\mathrm{BS}} = \frac{1}{C} \sum_{c=1}^{C} (\hat{\mathbf{p}}_i^c - \mathbf{y}_i^c)^2$$

We choose to report the ECE results for most of the experiments as ECE [12] is a widely used calibration metric.

D Analysis of Sample-Level Correspondence in PseudoCal

Analysis. Built upon the well-established *cluster assumption* [23, 67], we intuitively analyze how mixed samples can exhibit similar correct-wrong statistics as real target data, as empirically depicted in Figure 1(b). This assumption suggests that within a well-learned data structure, samples located far from the classification boundary are more likely to be correctly classified, while those near the boundary are prone to misclassification. While previous works often incorporate this assumption as an objective in model training [39, 68], our focus here is to employ it for explaining the inference behavior of a UDA model ϕ. We assume that the model has effectively learned the underlying target-domain structure. For simplicity, let's assume all involved labels in *mixup* are one-hot, and consider a fixed mix ratio λ noticeably greater than 0.5 (e.g., 0.65). This ensures a clear distinction between two involved real samples: one primary sample x_{t}^i with a mix ratio greater than 0.5, determining the mixed label y_{pt} for the mixed sample x_{pt}, and the other as the minor sample x_{t}^j, serving only as an input perturbation. If x_{pt} yields a correct model prediction $\hat{y}_{\mathrm{pt}}$ evaluated by its mixed label (i.e., $\hat{y}_{\mathrm{pt}} == y_{\mathrm{pt}}$), it suggests that the real sample x_{t}^i maintains its prediction after cross-cluster perturbation. This implies that x_{t}^i is likely distant from the classification boundary, and its prediction or pseudo-label $\hat{y}_{\mathrm{t}}^i$ is genuinely correct when evaluated against its ground truth y_{t}^i. Similarly, if x_{pt} yields a wrong model prediction $\hat{y}_{\mathrm{pt}}$ (i.e., $\hat{y}_{\mathrm{pt}} \neq y_{\mathrm{pt}}$), we can reasonably infer that x_{t}^i has a truly incorrect prediction. The presence of sample-level correspondence, when observed at the dataset level, manifests as similar correct-wrong statistics. However, this correspondence may not hold under extreme perturbation degrees (i.e., λ near 0.5 or 1.0).

In the above, we offer an intuitive analysis of the sample-level correspondence between pseudo-target data and real target samples. Figure 1(b) qualitatively illustrates the striking similarity in the correct-wrong statistics between the real target and pseudo target. To further enhance the understanding of this correspondence, we aim for a quantitative sample-level analysis. Consider a pair of real samples x_{t}^i with pseudo-label $\hat{y}_{\mathrm{t}}^i$ inferred by the UDA model ϕ, and x_{t}^j with pseudo-label $\hat{y}_{\mathrm{t}}^j$. We employ the *mixup* operation to generate a mixed sample x_{pt}^i with the mixed label y_{pt}^i. For simplicity, we assume that all labels are one-hot hard labels and λ is in the range of $(0.5, 1.0)$. This implies that x_{t}^i functions as the primary real sample, directly determining the mixed label y_{pt}^i, i.e., $y_{\mathrm{pt}}^i == \hat{y}_{\mathrm{t}}^i$. We apply the *mixup* operation n_{t} times during the model inference stage using unlabeled target data. This results in a labeled pseudo-target set $\{(x_{\mathrm{pt}}^i, y_{\mathrm{pt}}^i)\}_{i=1}^{n_{\mathrm{t}}}$ and the original pseudo-labeled real target set $\{(x_{\mathrm{t}}^i, \hat{y}_{\mathrm{t}}^i)\}_{i=1}^{n_{\mathrm{t}}}$. Using the same UDA model ϕ, we infer predictions $\hat{y}_{\mathrm{pt}}^i$ for the mixed sample x_{pt}^i and traverse through all mixed samples. For the mixed pseudo-target samples, we obtain predictions $\{\hat{y}_{\mathrm{pt}}^i\}_{i=1}^{n_{\mathrm{t}}}$ and corresponding labels $\{y_{\mathrm{pt}}^i\}_{i=1}^{n_{\mathrm{t}}}$. Regarding real target samples, the predictions are the available pseudo-labels $\{\hat{y}_{\mathrm{t}}^i\}_{i=1}^{n_{\mathrm{t}}}$, while the labels are ground truth labels $\{y_{\mathrm{t}}^i\}_{i=1}^{n_{\mathrm{t}}}$ which are used to assess the UDA model accuracy.

$$\mathrm{CR_{correct}} = \frac{\sum_i^{n_t}(\hat{y}^i_{\mathrm{pt}} == y^i_{\mathrm{pt}}) \cdot (\hat{y}^i_{\mathrm{t}} == y^i_{\mathrm{t}})}{\sum_i^{n_t}(\hat{y}^i_{\mathrm{t}} == y^i_{\mathrm{t}})} \tag{2}$$

$$\mathrm{CR_{wrong}} = \frac{\sum_i^{n_t}(\hat{y}^i_{\mathrm{pt}} \neq y^i_{\mathrm{pt}}) \cdot (\hat{y}^i_{\mathrm{t}} \neq y^i_{\mathrm{t}})}{\sum_i^{n_t}(\hat{y}^i_{\mathrm{t}} \neq y^i_{\mathrm{t}})} \tag{3}$$

$$\mathrm{CR_{arithmetic}} = \frac{\sum_i^{n_t}(\hat{y}^i_{\mathrm{pt}} == y^i_{\mathrm{pt}}) \cdot (\hat{y}^i_{\mathrm{t}} == y^i_{\mathrm{t}}) + \sum_i^{n_t}(\hat{y}^i_{\mathrm{pt}} \neq y^i_{\mathrm{pt}}) \cdot (\hat{y}^i_{\mathrm{t}} \neq y^i_{\mathrm{t}})}{n_{\mathrm{t}}} \tag{4}$$

$$\mathrm{CR_{harmonic}} = \frac{2 \cdot \mathrm{CR_{correct}} \cdot \mathrm{CR_{wrong}}}{\mathrm{CR_{correct}} + \mathrm{CR_{wrong}}} \tag{5}$$

Using these predictions and labels, we can systematically quantify the sample-level correspondence between the pseudo and real target sets for a more in-depth understanding. We establish such correspondence when both the predictions of a mixed pseudo sample and its primary real sample are either both correct or both wrong, as assessed by their respective labels. In other words, we consider a correspondence when $\hat{y}^i_{\mathrm{pt}} == y^i_{\mathrm{pt}}$ and $\hat{y}^i_{\mathrm{t}} == y^i_{\mathrm{t}}$, or when $\hat{y}^i_{\mathrm{pt}} \neq y^i_{\mathrm{pt}}$ and $\hat{y}^i_{\mathrm{t}} \neq y^i_{\mathrm{t}}$. To quantitatively measure this sample-level correspondence, we introduce four correspondence metrics. The first metric, denoted as $\mathrm{CR_{correct}}$, represents the correspondence rate of correct real samples (see Equation 2). It indicates how many correct real samples maintain correspondence with their mixed counterparts. Similarly, our second metric, denoted as $\mathrm{CR_{wrong}}$, measures the correspondence rate of wrong real samples (see Equation 3). For a more comprehensive perspective, we introduce the third metric, $\mathrm{CR_{arithmetic}}$, which calculates the arithmetic mean of $\mathrm{CR_{correct}}$ and $\mathrm{CR_{wrong}}$, assessing the correspondence rate of all real samples (see Equation 4). However, it's important to note that these three metrics may be misleading in extreme situations where most of the correspondences are biased toward either being correct or wrong. To address this issue, we propose our fourth metric, $\mathrm{CR_{harmonic}}$, which takes the harmonic mean of $\mathrm{CR_{correct}}$ and $\mathrm{CR_{wrong}}$, providing equal consideration to both correct and wrong correspondences (see Equation 5). This metric is inspired by the success of the H-Score solution in balanced accuracy measurement for known-unknown accuracy in open-set UDA, as demonstrated by previous studies [69, 70].

Table 5: By tuning the mix ratio λ, we can synthesize the most ambiguous pseudo samples ($\lambda = 0.51$) and the simplest ones ($\lambda = 1.0$), i.e., the pseudo-labeled real samples themselves. PseudoCal employs a moderate value of $\lambda = 0.65$ for all the results. Under these three cases, we measure the sample-level correspondence between the real samples and pseudo samples using four correspondence metrics.

Method	MCD		BNM		CDAN	SHOT	PADA		DINE
	D→A	W→A	Cl→Pr	Pr→Re	R→C	I→S	Ar→Cl	Re→Ar	P→R
No Calib. ECE (%)	16.39	17.03	22.09	15.72	9.83	34.71	20.35	8.31	12.39
PseudoCal (λ=1.0)	32.47	33.35	26.31	19.65	47.02	65.70	56.18	36.27	19.31
PseudoCal (λ=0.65)	**4.38**	**4.06**	**6.31**	**4.76**	**1.51**	**8.42**	**2.95**	**3.71**	**5.29**
PseudoCal (λ=0.51)	13.77	11.69	11.85	14.13	15.15	11.08	11.03	23.07	14.50
Oracle ECE (%)	2.31	1.90	3.14	1.10	1.28	4.39	2.16	2.87	1.29
Accuracy (%)	67.52	66.63	73.69	80.35	52.98	34.29	43.82	63.73	80.69
# of correct real data	1826	1792	3183	3408	9650	17218	703	656	55757
# of wrong real data	872	894	1135	836	8548	32998	918	385	13342
$\mathrm{CR_{harmonic}}$ (λ=1.0) (%)	0	0	0	0	0	0	0	0	0
$\mathrm{CR_{harmonic}}$ (λ=0.65) (%)	**63.45**	**63.45**	**59.89**	**59.27**	**60.56**	**56.28**	**60.21**	**62.04**	**61.73**
$\mathrm{CR_{harmonic}}$ (λ=0.51) (%)	52.08	54.42	53.13	52.87	45.33	35.18	50.94	46.03	56.26
$\mathrm{CR_{arithmetic}}$ (λ=1.0) (%)	**67.68**	**66.72**	**73.71**	**80.30**	53.03	34.29	43.37	**63.02**	**80.69**
$\mathrm{CR_{arithmetic}}$ (λ=0.65) (%)	62.36	62.75	61.72	63.08	**61.58**	65.58	**63.92**	61.00	70.73
$\mathrm{CR_{arithmetic}}$ (λ=0.51) (%)	52.07	54.10	50.03	47.51	56.35	**66.48**	63.02	50.52	50.74
$\mathrm{CR_{correct}}$ (λ=1.0) (%)	**100**	**100**	**100**	**100**	**100**	**100**	**100**	**100**	**100**
$\mathrm{CR_{correct}}$ (λ=0.65) (%)	59.93	61.16	63.52	65.22	52.09	44.48	50.74	56.02	75.11
$\mathrm{CR_{correct}}$ (λ=0.51) (%)	38.53	41.35	41.69	40.54	30.90	21.88	36.67	31.94	44.76
$\mathrm{CR_{wrong}}$ (λ=1.0) (%)	0	0	0	0	0	0	0	0	0
$\mathrm{CR_{wrong}}$ (λ=0.65) (%)	67.40	65.92	56.66	54.32	72.31	76.60	74.04	69.52	52.40
$\mathrm{CR_{wrong}}$ (λ=0.51) (%)	**80.32**	**79.57**	**73.2**	**75.99**	**85.04**	**89.75**	**83.38**	**82.39**	**75.73**

For empirical illustration, we conduct experiments using PseudoCal with varied λ values of $\{0.51, 0.65, 1.0\}$, among which 0.65 is our default value for all experiments in the main text. We report all results, including the measurement results of the sample-level correspondence using the four metrics described above, in Table 5. From the shown results, we can make three consistent observations: *(i)* As expected, only the harmonic metric $\mathrm{CR}_{\mathrm{harmonic}}$ is reliable and aligns with the actual calibration performance, while both the one-sided correct measure $\mathrm{CR}_{\mathrm{correct}}$ and the wrong measure $\mathrm{CR}_{\mathrm{wrong}}$ can be extremely biased, which would further directly mislead the arithmetic mean metric $\mathrm{CR}_{\mathrm{arithmetic}}$. *(ii)* In line with our discussion on the impact of mix ratio (λ), our observations reveal that λ values near 0.5 predominantly yield wrong predictions for pseudo-target samples (mixed samples), while λ values of 1.0 result in entirely correct predictions. The role of λ in controlling cross-cluster perturbation, determining the difficulty of mixed samples, is noteworthy. A λ close to 0.5 generates ambiguous mixed samples with almost even contributions from two real samples bearing different pseudo-labels. In such instances, the UDA model struggles to ascertain the class label, resulting in predominantly wrong predictions when evaluated with mixed labels. Conversely, a λ of 1.0 equates to not using *mixup* and directly leveraging pseudo-labeled real target samples. This scenario constitutes the easiest mixed samples, as the UDA model outputs predictions identical to raw target predictions, leading to entirely correct predictions when assessed with target pseudo-labels. From the *cluster assumption* perspective, extreme λ values render the relevant analysis inconclusive. A λ value very close to 0.5 makes it challenging to determine the primary real sample. Conversely, a λ value very close to 1.0 signifies the negligible cross-cluster perturbation, generating a mixed sample nearly identical to the primary real sample, wherein the cluster assumption does not apply. In general, extreme λ values, whether close to 0.5 or 1.0, exhibit significant bias towards either wrong or correct predictions, which indicates correct-wrong statistics of the pseudo-target set become skewed, deviating from real target samples. Hence, for a typical UDA model with both correct and wrong target predictions, we recommend employing a moderate λ value, such as the 0.65 utilized in our main text. *(iii)* Taking a closer look at the reliable measure of sample-level correspondence by $\mathrm{CR}_{\mathrm{harmonic}}$, we find that for various UDA models, there maintains a high correspondence with a $\mathrm{CR}_{\mathrm{harmonic}}$ value of about 60%, even for a low-accuracy model with only 30% accuracy. This strongly supports the robust existence of the *cluster assumption* and the robustness of our prior analysis. For a vivid illustration of the impact of λ values on sample-level correspondence, Figure 3 presents the correct-wrong statistics of all UDA methods outlined in Table 5. We find that extreme λ values result in a notable skewness in the correct-wrong statistics of the pseudo-target set when compared to the real target set. For a clear visualization of mixed images, please see Figure 4.

E Full Experiments

E.1 Settings

Datasets. For image classification, we adopt 5 popular UDA benchmarks of varied scales. *Office-31* [24] is a small-scale benchmark with 31 classes in 3 domains: Amazon (A), DSLR (D), and Webcam (W). *Office-Home* [25] is a medium-scale benchmark with 65 classes in 4 domains: Art (Ar), Clipart (Cl), Product (Pr), and Real-World (Re). *VisDA* [26] is a large-scale benchmark with over 200k images across 12 classes in 2 domains: Training (T) and Validation (V). *DomainNet* [27] is a large-scale benchmark with 600k images. We take a subset of 126 classes with 7 tasks[71] from 4 domains: Real (R), Clipart (C), Painting (P), and Sketch (S). *Image-Sketch* [28] is a large-scale benchmark with 1000 classes in 2 domains: ImageNet (I) and Sketch (S). For semantic segmentation, we use *Cityscapes*[29] as the target domain and either *GTA5*[30] or *SYNTHIA* [31] as the source.

UDA methods. We evaluate calibration on 10 UDA methods across 5 UDA scenarios. For image classification, we cover closed-set UDA methods (ATDOC [21], BNM [32], MCC [33], CDAN [5], SAFN [34], MCD [6]), partial-set UDA methods (ATDOC [21], MCC [33], PADA [10]), the whit-box source-free UDA method (SHOT [11]), and the black-box source-free UDA method (DINE [19]). For semantic segmentation, we focus on calibrating source-only models without any adaptation.

Calibration baselines. For a comprehensive comparison, we consider 5 typical calibration baselines in UDA, including the no calibration baseline (No Calib.), source-domain calibration (TempScal-src [12]), cross-domain calibration (CPCS [14], TransCal [16]), and a generic calibration method (Ensemble [13]).

Implementation details. We train all UDA models using their official code until convergence on a single RTX TITAN 16GB GPU. We adopt ResNet-101 [2] for *VisDA* and segmentation tasks, ResNet-34 [2] for *DomainNet*, and ResNet-50 [2] for all other tasks. For PseudoCal, a fixed mix ratio

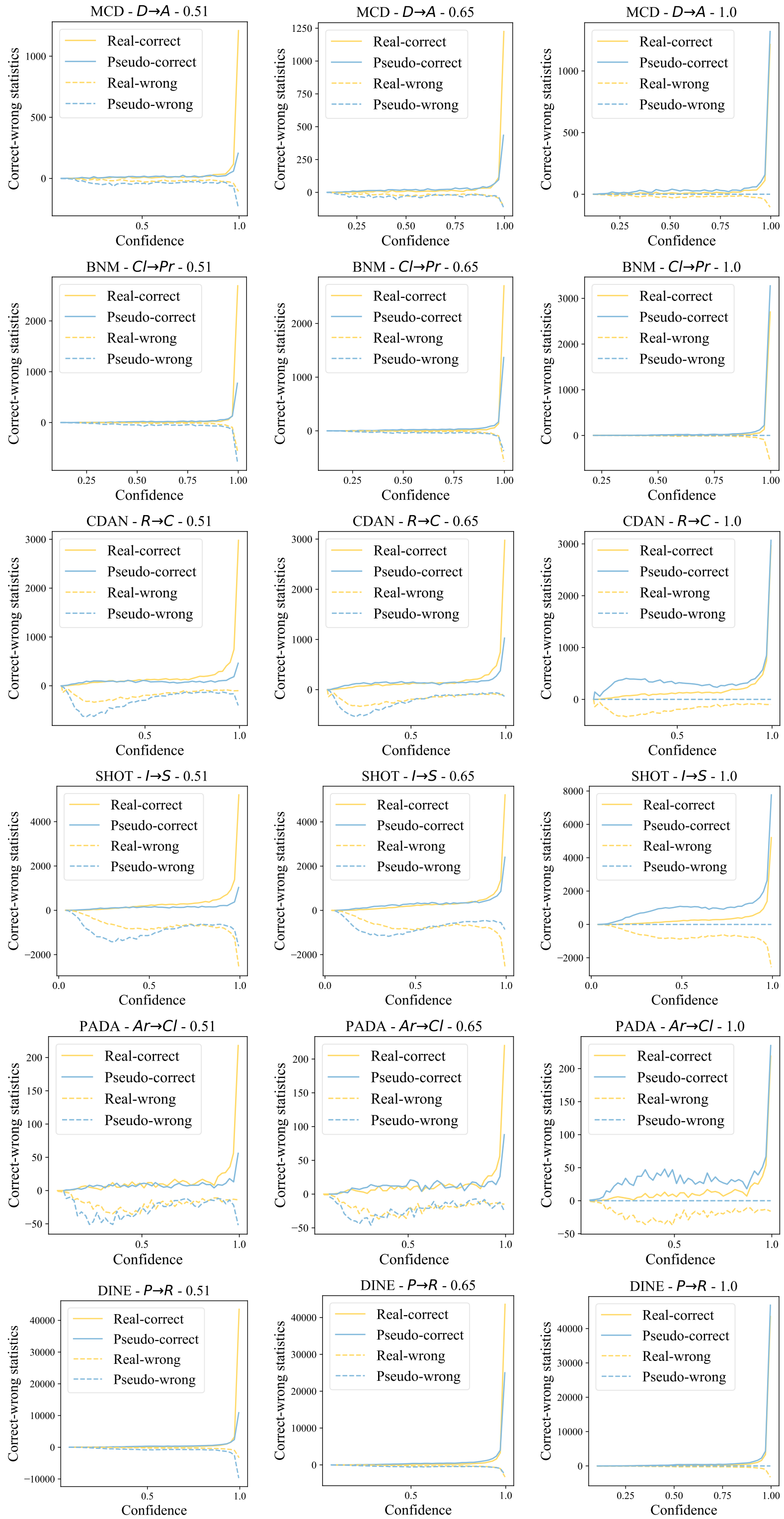

(a) $\lambda = 0.51$ (b) $\lambda = 0.65$ (c) $\lambda = 1.0$

Figure 3: The correct-wrong statistics are computed for both the pseudo-target and real target sets. We partition confidence values into 50 bins and present the count of correct and wrong predictions in each bin. Correctness for real target data is determined by comparing predictions of real target samples with ground truths. For pseudo-target data, correctness is assessed by comparing predictions of the mixed samples with mixed labels.

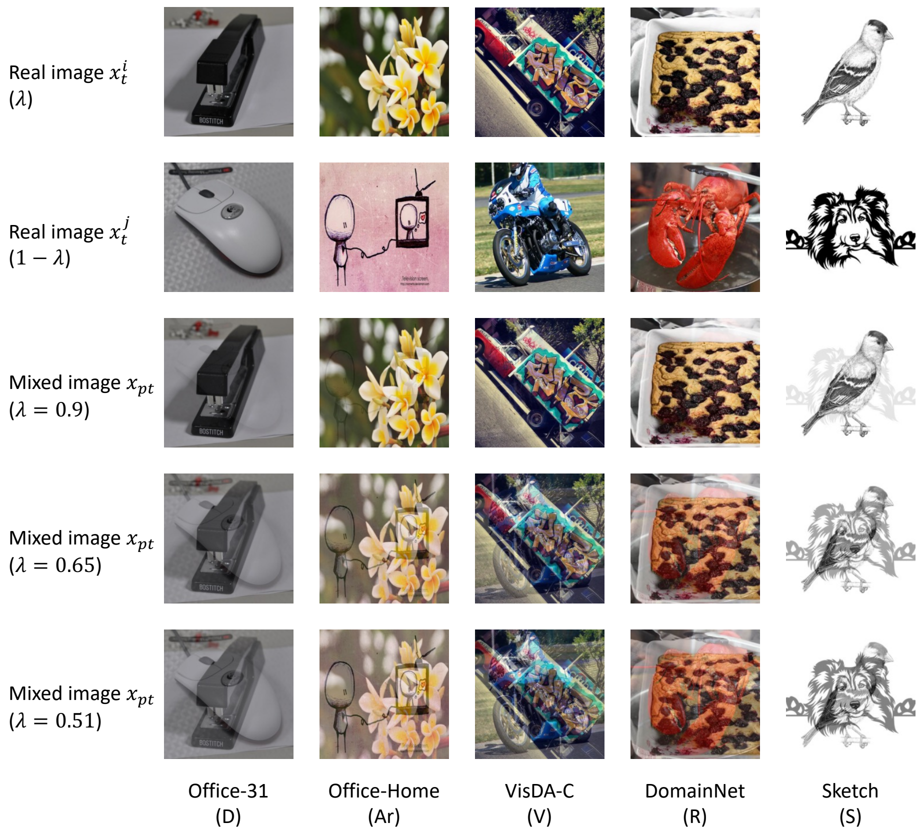

Figure 4: Visualization of input-level *mixup* for various UDA benchmarks with varied λ values.

λ of 0.65 is employed as default in all experiments. The UDA model is fixed for only inference use. We use it for one-epoch inference with *mixup* to generate the labeled pseudo-target set. The reported results are averaged over five random runs.

Table 6: ECE (%) of closed-set UDA on *Office-Home* (*Home*). Lower is better. **bold**: Best case.

Method	ATDOC					BNM					MCC				
	→Ar	→Cl	→Pr	→Re	avg	→Ar	→Cl	→Pr	→Re	avg	→Ar	→Cl	→Pr	→Re	avg
No Calib.	10.07	22.35	8.61	6.06	11.77	30.97	39.85	19.70	16.73	26.81	13.25	23.11	12.33	10.53	14.81
TempScal-src	6.19	17.54	**3.98**	**3.03**	7.68	23.11	30.32	13.70	10.25	19.35	6.74	16.25	**5.08**	4.10	8.04
CPCS	14.13	14.75	11.02	7.33	11.81	24.76	25.02	14.90	8.80	18.37	19.11	28.59	14.65	5.55	16.97
TransCal	18.09	6.52	16.03	18.29	14.73	17.44	27.22	9.14	5.47	14.82	11.73	3.86	6.70	8.16	7.61
Ensemble	7.38	18.01	5.51	4.22	8.78	22.50	30.68	14.38	12.53	20.02	9.76	19.20	9.48	7.90	11.58
PseudoCal (ours)	**2.42**	**2.93**	5.84	5.07	**4.07**	**17.34**	**16.03**	**6.20**	**4.68**	**11.06**	**2.85**	**2.25**	5.18	**3.57**	**3.47**
Oracle	1.71	1.91	2.29	1.69	1.90	2.20	2.53	2.36	1.60	2.17	2.25	1.64	2.22	1.91	2.00
Accuracy (%)	66.42	52.39	76.60	77.74	68.29	65.42	53.69	76.51	78.98	68.65	61.03	47.47	72.37	74.03	63.73

Method	CDAN					SAFN					MCD					*Home*
	→Ar	→Cl	→Pr	→Re	avg	→Ar	→Cl	→Pr	→Re	avg	→Ar	→Cl	→Pr	→Re	avg	AVG
No Calib.	13.38	22.94	12.15	10.00	14.62	16.57	27.90	13.16	11.93	17.39	16.36	25.96	13.29	11.97	16.89	17.05
TempScal-src	6.89	15.44	5.01	4.19	7.88	6.99	16.13	4.56	**4.07**	7.94	6.01	12.15	**3.56**	**3.54**	6.31	9.53
CPCS	18.38	33.56	15.29	9.90	19.28	14.98	30.54	10.06	12.11	16.92	25.13	27.26	10.17	14.29	19.21	17.09
TransCal	14.76	4.72	12.07	13.73	11.32	3.50	6.87	**3.77**	4.15	4.57	10.78	**2.66**	10.31	11.27	8.76	10.30
Ensemble	10.07	18.58	9.15	7.23	11.26	14.82	24.90	11.17	9.86	15.19	12.36	20.87	8.93	7.64	12.45	13.21
PseudoCal (ours)	**5.10**	**3.72**	**4.71**	**2.40**	**3.98**	**3.05**	**3.34**	6.86	4.37	**4.41**	**4.07**	2.86	6.26	3.72	**4.23**	**5.20**
Oracle	3.61	2.84	2.26	1.94	2.66	1.96	2.48	2.52	1.74	2.17	2.65	2.27	2.30	2.22	2.36	2.21
Accuracy (%)	62.26	49.99	71.19	73.79	64.31	65.84	51.90	73.78	75.09	66.66	59.04	46.80	68.75	71.39	61.49	65.52

E.2 Results

We evaluate PseudoCal across 5 UDA scenarios. For classification, we report the averaged ECE across UDA tasks sharing the same target domain in Tables 6-2. For segmentation, we take each

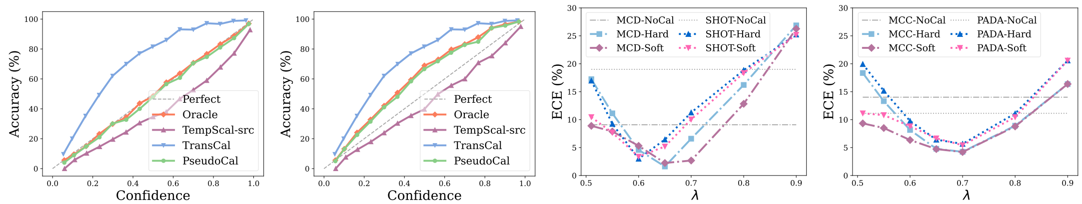

(a) CDAN on R $\rightarrow$ S (b) PADA on Ar $\rightarrow$ Cl (c) Closed-set on *DNet* (d) Partial-set on *Home*

Figure 5: (a) and (b) provide the reliability diagrams of various calibration methods for a qualitative comparison. (c) and (d) present the sensitivity analysis of the fixed mix ratio λ.

pixel as a sample and report the results in Table 9. 'Oracle' refers to the 'Oracle' calibration with target labels. 'Accuracy' (%) denotes the target accuracy of the fixed UDA model. For our calibration experiments on semantic segmentation, we calibrate the models trained solely on the source domain (GTA5 [30] or SYNTHIA [31]) without any target adaptation. We treat each pixel as an individual sample in classification tasks for both *mixup* and *temperature scaling*. To address the computational complexity, we adopt the evaluation strategy suggested in previous studies [56] and randomly sample 20,000 pixels from each image (with resolutions such as 1920*720) for calibration.

Closed-set UDA. We evaluate 6 UDA methods on 4 benchmarks for closed-set UDA. Specifically, we report the ECE for *Office-Home* in Table 6, ECE for both *Office-31* and *VisDA* in Table 7, and ECE for *DomainNet* in Table 1. PseudoCal consistently achieves a low ECE close to 'Oracle', significantly outperforming other calibration methods by a large margin. On the evaluated benchmarks, PseudoCal shows average ECE improvements of 4.33% on *Office-Home*, 1.88% on *Office-31*, 2.77% on *VisDA*, and 5.95% on *DomainNet* when compared to the second-best calibration method.

Table 7: ECE (%) of closed-set UDA on *Office-31* (*Office*) and *VisDA*.

Method	ATDOC →A	→D	→W	avg	T→V	BNM →A	→D	→W	avg	T→V	MCC →A	→D	→W	avg	T→V
No Calib.	12.17	4.59	6.66	7.81	10.38	23.41	11.12	8.27	14.27	17.10	19.29	6.18	7.80	11.09	17.42
TempScal-src	22.39	**3.39**	4.18	9.99	10.53	23.85	9.23	4.98	12.69	13.72	21.38	3.79	3.00	9.39	13.28
CPCS	24.64	7.98	8.94	13.85	16.65	22.45	11.65	**2.02**	12.04	15.36	30.16	4.69	3.03	12.63	7.14
TransCal	12.14	14.21	14.64	13.67	6.36	14.86	**5.22**	2.70	7.59	8.79	6.53	3.77	3.91	4.74	12.21
Ensemble	9.79	3.60	**4.09**	5.83	8.53	19.77	6.92	4.63	10.44	14.84	17.48	3.07	4.88	8.48	15.32
PseudoCal (ours)	**3.85**	6.64	4.98	**5.16**	**5.27**	**9.48**	6.30	3.97	**6.58**	**3.03**	**4.61**	**2.68**	**2.82**	**3.37**	**1.20**
Oracle	2.13	2.49	3.15	2.59	0.52	2.52	2.65	1.40	2.19	0.93	2.24	2.36	2.67	2.42	1.12
Accuracy (%)	73.23	91.57	88.93	84.58	75.96	72.56	88.35	90.94	83.95	76.23	69.69	91.37	89.06	83.37	78.00

Method	CDAN →A	→D	→W	avg	T→V	SAFN →A	→D	→W	avg	T→V	MCD →A	→D	→W	avg	T→V	*Office* AVG	*VisDA* AVG
No Calib.	17.02	9.34	7.96	11.44	15.90	21.34	6.17	6.68	11.40	18.53	16.71	9.49	8.88	11.69	17.58	11.28	16.15
TempScal-src	18.54	5.70	3.41	9.21	14.19	23.95	3.21	2.83	9.99	14.40	25.37	**3.44**	**2.36**	10.39	10.22	10.28	12.72
CPCS	17.47	30.95	5.67	18.03	15.45	23.15	8.21	18.21	16.52	17.88	27.69	11.85	19.01	19.52	10.56	15.43	13.84
TransCal	**4.84**	7.44	6.84	6.38	4.07	8.14	**3.04**	2.81	**4.67**	8.23	5.13	5.65	4.76	5.18	**3.74**	7.04	7.23
Ensemble	10.92	4.98	3.29	6.40	13.30	18.89	3.81	5.75	9.48	17.31	14.56	6.25	5.49	8.77	14.82	8.23	14.02
PseudoCal (ours)	6.58	**4.78**	**3.04**	**4.80**	**3.04**	**4.13**	7.92	5.51	5.85	**7.54**	**4.22**	5.97	5.33	**5.17**	6.71	**5.16**	**4.46**
Oracle	3.21	3.26	2.17	2.88	1.00	2.21	2.90	1.75	2.29	1.82	2.11	3.55	1.76	2.47	0.99	2.47	1.06
Accuracy (%)	66.03	87.15	87.17	80.12	75.24	68.95	89.96	88.55	82.49	73.91	67.07	86.14	85.53	79.58	72.18	82.35	75.25

Table 8: ECE (%) of partial-set UDA on *Office-Home* (*Home*).

Method	ATDOC →Ar	→Cl	→Pr	→Re	avg	MCC →Ar	→Cl	→Pr	→Re	avg	PADA →Ar	→Cl	→Pr	→Re	avg	*Home* AVG
No Calib.	16.68	28.47	20.00	12.26	19.35	12.71	22.17	12.21	8.99	14.02	9.45	19.09	9.19	6.77	11.13	14.83
TempScal-src	13.40	24.79	14.91	8.72	15.45	7.12	15.97	6.04	**4.35**	8.37	8.92	18.20	6.21	4.08	9.35	11.06
CPCS	19.39	29.74	13.86	14.63	19.41	12.73	28.11	9.09	10.69	15.16	24.40	22.74	17.30	27.67	23.03	19.20
TransCal	10.64	**5.17**	**5.88**	11.30	8.25	9.44	4.27	**5.41**	6.98	6.53	22.70	11.00	23.00	26.77	20.87	11.88
Ensemble	11.98	21.28	13.44	8.62	13.83	9.22	18.54	10.11	6.78	11.16	5.30	11.86	**4.43**	**3.92**	**6.38**	10.46
PseudoCal (ours)	**7.87**	10.90	6.24	**4.83**	**7.46**	**3.74**	**3.63**	6.93	4.81	**4.78**	**4.72**	**3.45**	10.77	6.69	6.41	**6.22**
Oracle	4.13	4.45	4.37	4.08	4.26	2.81	3.01	3.06	2.37	2.81	3.94	2.65	4.80	3.03	3.61	3.56
Accuracy (%)	63.02	50.70	65.92	73.71	63.34	65.53	51.68	73.41	78.23	67.21	55.65	44.06	61.23	66.54	56.87	62.47

Partial-set UDA. We evaluate 3 partial-set UDA methods on *Office-Home* and report the ECE in Table 8. PseudoCal consistently performs the best on average and outperforms the second-best method (Ensemble) by a significant margin of 4.24%.

Source-free UDA. We evaluate source-free UDA settings using SHOT and DINE. We report the ECE for *DomainNet* and *Image-Sketch* together in Table 2. PseudoCal outperforms Ensemble on both benchmarks by significant margins, with 7.44% on *DomainNet* and 15.05% on *Image-Sketch*.

Method	*GTA5* [30]	*SYNTHIA* [31]	AVG
No Calib.	7.87	23.08	15.48
TempScal-src	4.61	19.24	11.93
Ensemble	**2.66**	20.84	11.75
PseudoCal (ours)	5.73	**15.99**	**10.86**
Oracle	0.52	4.5	2.51

Table 9: ECE (%) of segmentation.

Method	ECE [12] (%)	BS [66]	NLL [65]
No Calib.	11.52	0.5674	1.9592
TempScal-src	10.63	0.5647	1.9418
CPCS	5.48	0.5579	1.8781
TransCal	23.38	0.6279	2.1089
Ensemble	10.08	0.5618	1.9260
PseudoCal (ours)	**3.63**	**0.5553**	**1.8697**
Oracle	1.29	0.5519	1.8597

Table 10: ViT results of MCC on C$\to$S.

Semantic segmentation. In addition to assessing the performance of PseudoCal in classification tasks, we also evaluate PseudoCal on the domain adaptive semantic segmentation tasks and report the ECE in Table 9. Remarkably, PseudoCal performs the best on average and demonstrates an average ECE improvement of 4.62% over the no-calibration baseline.

E.3 Discussion

Qualitative comparisons. Reliability diagrams in Figure 5(a)-(b) show that PseudoCal consistently aligns with 'Oracle', while the existing state-of-the-art method TransCal deviates significantly.

Impact of mix ratio λ. The fixed mix ratio λ is the sole hyperparameter in PseudoCal. We investigate its impact on calibration performance by experimenting with values ranging from 0.51 to 0.9. The results of two closed-set UDA methods (including SHOT) on *DomainNet* are presented in Figure 5(c), and the results of two partial-set UDA methods on *Office-Home* are shown in Figure 5(d). We first examine *mixup* with both 'Hard' (one-hot labels) and 'Soft' (soft predictions) labels, finding similar trends with differences that are generally not visible when $\lambda > 0.6$. In addition, optimal performance for PseudoCal occurs with a moderate λ value between 0.6 and 0.7. The reason for this is that a λ value closer to 0.5 generates more ambiguous samples, resulting in increased wrong predictions, whereas a λ value closer to 1.0 has the opposite effect. For more details, kindly refer to Appendix D, where we examine the impact of different λ values on the sample-level correspondence. At last, for simplicity, we use a fixed λ value of 0.65 as default with hard labels for all experiments.

Impact of backbones and metrics. In order to examine the robustness of PseudoCal across different backbones and calibration metrics, we assess its performance using ViT-B [3] as the backbone and present the results for the aforementioned three metrics in Table 10. The findings reveal that PseudoCal consistently achieves the best performance regardless of the choice of backbone or calibration metric.

Impact of UDA model quality. We've provided the target-domain accuracy for each UDA model in the 'Accuracy' row. PseudoCal remains effective as long as the UDA model has learned the target data structure instead of being completely randomly initialized, supported by the robust *cluster assumption*. This is evident in Table 2, where PseudoCal maintains its competence even with low accuracy pseudo-labels (about 30%).

Comparison with training-stage *mixup*. Most approaches incorporate *mixup* [22] during the model training stage as an objective to enhance model generalization, and among them, [62] further utilizes *mixup* as a training-stage calibration method. However, our use of *mixup* in PseudoCal differs significantly from previous *mixup*-based works in three key aspects. *(i)* Different stages: All of these works apply *mixup* in training, while our *mixup* operation occurs in the inference stage to synthesize a labeled set. *(ii)* Different mix ratios: PseudoCal leverages *mixup* for cross-cluster sample interpolation and performs effectively with a fixed mix ratio $\lambda \in (0.6, 0.7)$ but is considerably less effective with λ values close to 1.0. In contrast, previous methods typically work best with $\lambda \in \text{Beta}(\alpha, \alpha)$ where $\alpha \in [0.1, 0.4]$, essentially favoring λ values that are close to 1.0. However, they are ineffective with λ values close to 0.5 (like our adopted values) due to the manifold intrusion problem [62, 72]. *(iii)* Different performance: We observed that UDA models trained with training-time calibration methods still suffer from significant miscalibration, while our PseudoCal can further substantially reduce ECE errors for these models. For example, as shown in Table 2, SHOT employs *label smoothing*[73, 63] during training, and DINE is trained with *mixup*[62, 68].

Ablation study on pseudo-target synthesis. Pseudo-target synthesis plays a critical role in our PseudoCal framework. In this step, we employ input-level *mixup* with a fixed mix ratio (λ) to

Table 11: ECE (%) of ablation experiments on pseudo-target synthesis.

Method	MCD		BNM		CDAN	SHOT	PADA		DINE
	D→A	W→A	Cl→Pr	Pr→Re	R→C	I→S	Ar→Cl	Re→Ar	P→R
No Calib.	16.39	17.03	22.09	15.72	9.83	34.71	20.35	8.31	12.39
MocoV2Aug [74]	16.85	17.21	20.51	14.98	15.49	28.63	25.81	15.17	11.12
RandAug [75]	12.87	11.53	19.24	11.37	13.33	29.28	18.47	10.32	12.62
CutMix [76]	8.20	6.39	14.82	10.60	7.60	23.18	15.96	6.04	6.93
ManifoldMix [77]	19.49	19.27	23.29	16.94	27.00	50.54	36.04	21.29	16.88
Mixup-Beta [22]	14.96	13.11	15.65	11.24	15.84	26.74	23.85	11.46	9.72
Pseudo-Label [78]	32.47	33.35	26.31	19.65	47.02	65.70	56.18	36.27	19.31
Filtered-PL [79]	31.74	32.73	26.14	19.46	45.35	64.29	54.83	35.10	19.05
PseudoCal-same	19.31	20.54	22.50	15.63	25.43	45.54	30.30	18.46	15.56
PseudoCal (ours)	**4.38**	**4.06**	**6.31**	**4.76**	**1.51**	**8.42**	**2.95**	**3.71**	**5.29**
Oracle	2.31	1.90	3.14	1.10	1.28	4.39	2.16	2.87	1.29
Accuracy (%)	67.52	66.63	73.69	80.35	52.98	34.29	43.82	63.73	80.69

generate a pseudo-target sample by combining two real samples with different pseudo-labels. We conduct a comprehensive ablation study on this synthesis strategy by extensively comparing it with alternative approaches, including: *(i)* Applying *mixup* between samples with the same pseudo-label (referred to as PseudoCal-same). *(ii)* Using instance-based augmentations of target samples, such as RandAugment [75], and strong augmentations commonly used in self-supervised learning [74]. *(iii)* Employing *mixup* at different levels, such as the patch-level [76] and the feature-level [77]. *(iv)* Applying common training-stage *mixup* using $\lambda \in \text{Beta}(0.3, 0.3)$ [22]. *(v) Directly utilizing original or filtered pseudo-labeled real target samples [78, 79] without mixup (by setting the mix ratio λ to* 1.0*).* We present an extensive comparison of all these strategies in Table 11. The results consistently demonstrate that our inference-stage input-level *mixup* outperforms the alternative options.

Table 12: ECE (%) of calibration results when combining PseudoCal with different supervised calibration methods, including MatrixScal [12], VectorScal [12], and TempScal [12] (our default choice).

Method	MCD		BNM		CDAN	SHOT	PADA		DINE
	D→A	W→A	Cl→Pr	Pr→Re	R→C	I→S	Ar→Cl	Re→Ar	P→R
No Calib.	16.39	17.03	22.09	15.72	9.83	34.71	20.35	8.31	12.39
MatrixScal-src	17.86	20.28	25.73	15.98	22.11	-	36.55	20.45	-
VectorScal-src	17.75	20.52	16.40	12.36	12.88	-	20.53	9.07	-
TempScal-src	32.09	18.65	15.10	11.64	9.27	-	15.15	6.34	-
PseudoCal(Matrix.)	11.61	13.20	16.07	11.83	15.09	42.86	35.85	27.07	7.65
PseudoCal(Vector.)	11.00	9.32	9.31	6.05	6.37	23.90	5.90	4.19	6.23
PseudoCal(Temp.)	**4.38**	**4.06**	**6.31**	**4.76**	**1.51**	**8.42**	**2.95**	**3.71**	**5.29**
Oracle	2.31	1.90	3.14	1.10	1.28	4.39	2.16	2.87	1.29
Accuracy (%)	67.52	66.63	73.69	80.35	52.98	34.29	43.82	63.73	80.69

Compatibility with other supervised calibration methods. As *matrix scaling* (MatrixScal), *vector scaling* (VectorScal), and *temperature scaling* (TempScal) are similar, all proposed by [12], and the authors have demonstrated that *temperature scaling* (TempScal) is the superior solution. Therefore, as for the source-domain calibration baseline (using a labeled source validation set for calibration), we have only reported the results of TempScal-src in the tables in the main text. Here, we present the results of MatrixScal-src and VectorScal-src for additional reference, without impacting any of the conclusions drawn in the main text. While our PseudoCal is inspired by the factorized NLL of TempScal and naturally employs TempScal as the default supervised calibration method for our synthesized labeled pseudo-target set, we investigate the compatibility of PseudoCal with alternative supervised calibration methods, such as MatrixScal and VectorScal. The corresponding results are detailed in Table 12. Our findings reveal two key observations: *(i)* If a supervised calibration method exhibits stability and effectiveness with the source labeled data, combining it with PseudoCal tends to yield reduced ECE error compared to the no calibration baseline. *(ii)* Due to the similarity in correct-wrong statistics between the pseudo-target set and real target data, PseudoCal demonstrates compatibility with both MatrixScal and VectorScal. However, it consistently achieves the best calibration performance when paired with TempScal, aligning with the conclusion in [12] that TempScal generally outperforms MatrixScal and VectorScal.

Limitations. PseudoCal has the following limitations and potential negative societal impacts: (*i*) Like other calibration methods compared, PseudoCal may occasionally increase ECE when the initial ECE is already small (see →D in Table 7), which raises risks for safety-critical decision-making systems. (*ii*) PseudoCal may face challenges in extreme cases with very few available unlabeled target samples, such as only a small batch of samples or even a single target sample. (*iii*) PseudoCal is partly dependent on the *cluster assumption*, and it may fail if the target pseudo label is extremely poor, i.e., performing similarly to random trials.

E.4 Task-Level Results

We have presented the average results for tasks with the same target domain. For example, in the case of *Office-Home*, UDA tasks including 'Cl→Ar', 'Pr→Ar', and 'Re→Ar' share the common target domain 'Ar'. Consequently, we have averaged the results of these three UDA tasks and reported the averaged value in the tables within our main text under the row labeled '→ Ar'. Additionally, note that the 'avg' row represents the averaged results within each UDA method's rows to the left of the 'avg' row. Differently, the 'AVG' row signifies the averaged results across all 'avg' rows associated with different UDA methods. Consequently, the 'AVG' row can be considered more reliable and representative for drawing conclusions. For detailed calibration results for each task, please refer to Table 13 through Table 31.

Table 13: ECE (%) of a closed-set UDA method ATDOC [21] on *Office-Home*.

Method	Ar → Cl	Ar → Pr	Ar → Re	Cl → Ar	Cl → Pr	Cl → Re	Pr → Ar	Pr → Cl	Pr → Re	Re → Ar	Re → Cl	Re → Pr	avg
No Calib.	22.83	10.57	6.31	10.77	8.88	6.38	10.39	22.61	5.49	9.06	21.61	6.38	11.77
MatrixScal-src	35.03	20.72	18.28	27.54	24.73	23.40	22.51	32.85	13.66	20.25	32.89	12.90	23.73
VectorScal-src	22.05	10.09	5.85	11.51	7.74	6.01	15.12	26.85	7.81	7.94	21.10	5.03	12.26
TempScal-src	14.69	5.55	**2.60**	4.27	**3.17**	**1.45**	9.67	22.55	5.04	4.63	15.37	**3.21**	7.68
CPCS	8.37	9.32	6.44	12.94	14.94	11.41	12.28	6.00	4.13	17.18	29.88	8.80	11.81
TransCal	4.95	13.85	16.58	17.29	17.34	18.76	18.77	7.48	19.54	18.20	7.13	16.90	14.73
Ensemble	18.40	7.47	4.51	7.82	4.76	4.24	8.36	17.96	**3.92**	5.96	17.68	4.29	8.78
PseudoCal	**3.07**	**4.23**	5.28	**1.96**	6.27	5.70	**2.52**	**4.05**	4.22	**2.79**	**1.68**	7.03	**4.07**
Oracle	2.38	3.14	2.34	1.44	1.92	1.36	1.98	1.92	1.37	1.71	1.43	1.80	1.90
Accuracy (%)	52.07	74.48	79.27	64.24	73.85	75.42	64.65	50.65	78.54	70.37	54.46	81.48	68.29

Table 14: ECE (%) of a closed-set UDA method BNM [32] on *Office-Home*.

Method	Ar → Cl	Ar → Pr	Ar → Re	Cl → Ar	Cl → Pr	Cl → Re	Pr → Ar	Pr → Cl	Pr → Re	Re → Ar	Re → Cl	Re → Pr	avg
No Calib.	38.64	22.49	16.21	30.89	22.09	18.25	34.90	42.46	15.72	27.11	38.44	14.52	26.81
MatrixScal-src	39.37	23.31	19.01	30.30	25.73	22.24	31.37	41.37	15.98	24.06	37.39	14.77	27.07
VectorScal-src	30.83	17.66	9.97	21.91	16.40	11.46	27.76	37.27	12.36	18.91	29.06	10.03	20.30
TempScal-src	27.22	16.34	8.91	20.39	15.10	10.21	28.82	35.60	11.64	20.12	28.15	9.67	19.35
CPCS	33.80	18.08	8.12	17.24	19.77	7.90	28.68	**17.28**	10.39	28.36	23.97	6.86	18.37
TransCal	25.75	12.11	5.87	15.73	10.51	5.51	21.41	29.66	5.02	**15.17**	26.25	4.80	14.82
Ensemble	29.52	16.03	12.00	22.77	15.55	14.06	25.17	32.06	11.53	19.55	30.46	11.56	20.02
PseudoCal	**14.27**	**8.74**	**4.60**	**15.46**	**6.31**	**4.69**	**20.90**	18.35	**4.76**	15.66	**15.47**	**3.55**	**11.06**
Oracle	3.16	2.18	1.76	2.00	3.14	1.95	2.92	1.78	1.10	1.68	2.64	1.77	2.17
Accuracy (%)	54.39	73.49	79.78	64.52	73.69	76.82	61.68	51.13	80.35	70.05	55.56	82.36	68.65

Table 15: ECE (%) of a closed-set UDA method MCC [33] on *Office-Home*.

Method	Ar → Cl	Ar → Pr	Ar → Re	Cl → Ar	Cl → Pr	Cl → Re	Pr → Ar	Pr → Cl	Pr → Re	Re → Ar	Re → Cl	Re → Pr	avg
No Calib.	23.74	14.31	10.89	12.70	13.15	11.72	14.36	23.18	8.98	12.69	22.40	9.54	14.81
MatrixScal-src	37.39	23.28	19.95	31.00	27.75	25.27	26.13	35.70	16.27	21.56	35.20	14.95	26.20
VectorScal-src	21.05	12.79	7.87	10.96	11.18	8.20	16.87	28.29	9.64	7.58	21.40	6.15	13.50
TempScal-src	12.23	6.43	3.61	4.06	4.69	**2.85**	11.38	22.91	5.83	4.79	13.60	**4.11**	8.04
CPCS	25.11	15.31	**3.60**	19.41	14.36	4.49	13.83	35.66	8.56	24.08	24.99	14.27	16.97
TransCal	3.04	6.31	5.98	12.75	7.42	8.60	11.95	4.59	9.90	10.48	3.95	6.37	7.61
Ensemble	19.20	11.30	8.05	10.01	9.69	8.51	10.11	18.98	7.13	9.15	19.42	7.44	11.58
PseudoCal	**2.71**	**5.04**	3.81	**3.17**	**4.64**	3.06	**2.66**	**1.54**	**3.85**	**2.73**	**2.51**	5.86	**3.47**
Oracle	2.41	2.57	2.31	2.67	1.73	1.62	1.58	0.84	1.80	2.51	1.66	2.35	2.00
Accuracy (%)	47.26	69.29	75.90	59.91	68.33	70.16	56.32	44.49	76.04	66.87	50.65	79.48	63.73

Table 16: ECE (%) of a closed-set UDA method CDAN [5] on *Office-Home*.

Method	Ar → Cl	Ar → Pr	Ar → Re	Cl → Ar	Cl → Pr	Cl → Re	Pr → Ar	Pr → Cl	Pr → Re	Re → Ar	Re → Cl	Re → Pr	avg
No Calib.	24.88	14.66	10.39	14.71	13.05	11.25	13.24	22.54	8.37	12.19	21.41	8.74	14.62
MatrixScal-src	35.03	22.64	19.14	28.14	26.14	22.96	24.20	33.34	15.03	20.32	30.69	13.78	24.28
VectorScal-src	18.81	10.46	7.24	8.92	9.81	6.73	15.31	26.51	9.18	7.51	16.70	5.76	11.91
TempScal-src	12.48	5.82	3.40	**5.57**	5.14	3.06	9.78	21.29	6.12	5.31	12.55	**4.06**	7.88
CPCS	31.45	13.21	2.36	25.84	24.68	17.24	13.44	27.86	10.09	15.85	41.38	7.98	19.28
TransCal	**2.65**	11.04	11.67	14.44	13.41	14.01	16.34	6.04	15.50	13.51	5.46	11.77	11.32
Ensemble	18.64	11.85	7.23	10.87	9.04	7.94	9.45	19.12	6.52	9.90	17.97	6.56	11.26
PseudoCal	3.52	**4.33**	**2.32**	5.67	**4.81**	**2.82**	**6.36**	**3.78**	**2.05**	**3.28**	**3.85**	5.00	**3.98**
Oracle	1.83	2.96	1.94	3.88	1.74	2.20	4.46	3.22	1.68	2.50	3.48	2.08	2.66
Accuracy (%)	48.00	67.00	75.07	59.83	66.88	69.98	58.59	48.64	76.31	68.36	53.33	79.68	64.31

Table 17: ECE (%) of a closed-set UDA method SAFN [34] on *Office-Home*.

Method	Ar → Cl	Ar → Pr	Ar → Re	Cl → Ar	Cl → Pr	Cl → Re	Pr → Ar	Pr → Cl	Pr → Re	Re → Ar	Re → Cl	Re → Pr	avg
No Calib.	28.25	15.29	12.40	16.62	14.10	12.45	18.17	29.68	10.94	14.92	25.77	10.08	17.39
MatrixScal-src	37.63	23.66	20.05	28.07	26.01	23.00	25.60	37.84	16.22	20.98	33.18	14.69	25.58
VectorScal-src	21.01	12.78	9.20	10.96	10.28	7.67	16.03	26.93	8.91	10.72	20.21	6.35	13.42
TempScal-src	12.33	5.56	3.17	4.62	4.22	**3.40**	9.99	21.72	5.64	6.36	14.33	3.89	7.94
CPCS	31.45	16.18	10.90	23.93	11.19	6.71	15.78	25.66	18.73	5.24	34.50	**2.80**	16.92
TransCal	7.50	**4.23**	**2.80**	4.11	**3.63**	4.89	3.14	7.47	4.76	3.26	5.65	3.46	4.57
Ensemble	25.00	13.33	9.91	15.20	11.62	10.14	16.12	26.14	9.54	13.15	23.56	8.55	15.19
PseudoCal	**3.30**	6.41	4.14	**3.46**	7.06	5.18	**2.99**	**3.40**	**3.79**	**2.70**	**3.33**	7.12	**4.41**
Oracle	3.10	3.78	1.94	2.06	1.85	2.18	2.65	1.66	1.11	1.16	2.68	1.92	2.17
Accuracy (%)	50.65	70.96	75.81	64.44	70.42	72.30	62.55	49.55	77.16	70.54	55.51	79.97	66.66

Table 18: ECE (%) of a closed-set UDA method MCD [6] on *Office-Home*.

Method	Ar → Cl	Ar → Pr	Ar → Re	Cl → Ar	Cl → Pr	Cl → Re	Pr → Ar	Pr → Cl	Pr → Re	Re → Ar	Re → Cl	Re → Pr	avg
No Calib.	26.24	16.26	12.30	16.42	14.19	13.27	19.02	27.38	10.35	13.63	24.25	9.43	16.89
MatrixScal-src	41.44	28.57	22.89	34.21	27.91	26.19	28.46	39.91	18.20	22.91	36.82	16.58	28.67
VectorScal-src	21.79	12.62	8.36	11.89	7.19	7.75	17.75	27.43	8.99	10.10	20.83	5.72	13.37
TempScal-src	8.59	**4.59**	**2.87**	3.65	**2.79**	**2.90**	10.42	17.99	4.85	3.96	9.86	**3.29**	6.31
CPCS	20.66	11.43	21.72	27.95	11.22	11.03	24.03	12.63	10.13	23.42	48.48	7.86	19.21
TransCal	**2.43**	8.94	9.45	10.78	10.81	10.80	9.86	**2.07**	13.56	11.69	3.49	11.19	8.76
Ensemble	20.49	10.59	7.24	11.59	9.53	9.16	15.53	22.66	6.52	9.95	19.45	6.66	12.45
PseudoCal	2.52	4.93	3.93	**3.39**	6.57	3.70	**5.05**	2.68	**3.52**	**3.76**	**3.39**	7.28	**4.23**
Oracle	2.22	2.48	2.08	2.68	2.31	2.13	3.02	1.97	2.44	2.26	2.61	2.11	2.36
Accuracy (%)	46.55	63.75	73.01	57.44	64.86	67.45	53.81	42.77	73.72	65.88	51.07	77.63	61.49

Table 19: ECE (%) of a closed-set UDA method ATDOC [21] on *DomainNet*.

Method	C → S	P → C	P → R	R → C	R → P	R → S	S → P	avg
No Calib.	12.22	9.27	3.75	9.81	6.85	12.36	7.92	8.88
MatrixScal-src	34.30	27.58	15.58	23.23	18.37	28.05	27.44	24.94
VectorScal-src	16.19	11.45	3.97	15.11	10.19	19.26	9.52	12.24
TempScal-src	10.32	6.52	1.94	10.86	8.51	13.31	6.92	8.34
CPCS	12.87	13.31	4.46	8.25	5.11	13.90	4.34	8.89
TransCal	19.89	23.51	26.65	22.52	24.93	19.46	24.59	23.08
Ensemble	8.71	5.73	**1.59**	6.91	4.41	9.38	4.66	5.91
PseudoCal	**1.68**	**1.98**	2.51	**1.66**	**1.21**	**1.71**	**1.61**	**1.77**
Oracle	0.98	1.92	0.86	1.18	0.70	1.16	1.17	1.14
Accuracy (%)	53.74	56.51	74.95	55.59	61.65	50.41	59.64	58.93

Table 20: ECE (%) of a closed-set UDA method BNM [32] on *DomainNet*.

Method	C → S	P → C	P → R	R → C	R → P	R → S	S → P	avg
No Calib.	30.88	29.27	15.37	27.87	21.79	31.65	22.41	25.61
MatrixScal-src	37.91	31.17	18.31	26.82	22.33	32.31	28.64	28.21
VectorScal-src	23.10	20.02	9.88	21.80	14.83	26.68	14.18	18.64
TempScal-src	19.11	18.79	9.40	19.28	14.42	21.49	12.81	16.47
CPCS	14.45	13.75	7.98	**2.72**	4.35	**4.14**	11.50	8.41
TransCal	9.21	**6.31**	**5.82**	6.73	**1.69**	9.56	**1.98**	**5.90**
Ensemble	25.08	23.46	12.61	23.42	18.52	27.34	18.70	21.30
PseudoCal	**5.08**	12.43	6.18	8.10	5.20	6.64	6.82	7.21
Oracle	1.60	3.17	3.40	1.63	1.50	1.00	1.81	2.02
Accuracy (%)	52.90	55.52	74.30	57.71	63.95	51.61	62.30	59.76

Table 21: ECE (%) of a closed-set UDA method MCC [33] on *DomainNet*.

Method	C → S	P → C	P → R	R → C	R → P	R → S	S → P	avg
No Calib.	15.19	8.29	4.79	8.98	6.91	12.04	8.63	9.26
MatrixScal-src	36.95	28.60	15.99	23.92	18.95	29.54	28.72	26.10
VectorScal-src	18.52	11.63	4.49	15.98	10.72	20.86	10.71	13.27
TempScal-src	13.49	5.92	**2.36**	10.83	8.96	14.27	7.67	9.07
CPCS	29.26	15.02	3.44	3.03	6.00	5.15	2.66	9.22
TransCal	16.89	22.54	23.45	22.00	24.68	19.17	23.44	21.74
Ensemble	11.36	5.38	2.57	6.03	4.40	9.32	5.80	6.41
PseudoCal	**2.72**	**1.45**	2.38	**1.25**	**1.64**	**3.48**	**2.13**	**2.15**
Oracle	0.80	1.36	1.09	0.96	1.18	0.97	1.70	1.15
Accuracy (%)	47.65	51.27	71.62	50.51	59.02	45.14	56.46	54.52

Table 22: ECE (%) of a closed-set UDA method CDAN [5] on *DomainNet*.

Method	C → S	P → C	P → R	R → C	R → P	R → S	S → P	avg
No Calib.	17.00	10.51	5.56	9.83	8.26	11.88	11.03	10.58
MatrixScal-src	35.28	27.82	15.80	22.11	18.34	27.24	27.76	24.91
VectorScal-src	17.44	10.88	4.37	12.88	9.45	17.90	9.81	11.82
TempScal-src	13.39	6.58	2.75	9.27	8.30	11.22	8.32	8.55
CPCS	**2.40**	17.27	5.57	4.24	6.75	11.42	**1.81**	7.07
TransCal	14.85	20.65	22.93	21.19	22.27	19.01	20.55	20.21
Ensemble	12.96	7.47	3.54	6.96	5.73	9.62	7.75	7.72
PseudoCal	3.48	**1.65**	**1.86**	**1.51**	**1.70**	**1.85**	2.08	**2.02**
Oracle	1.03	1.61	1.07	1.28	0.73	0.84	1.43	1.14
Accuracy (%)	49.07	53.25	71.82	52.98	60.75	49.11	57.51	56.36

Table 23: ECE (%) of a closed-set UDA method SAFN [34] on *DomainNet*.

Method	C → S	P → C	P → R	R → C	R → P	R → S	S → P	avg
No Calib.	21.82	17.98	10.15	17.90	13.63	20.70	15.25	16.78
MatrixScal-src	33.45	22.54	11.16	21.05	15.53	26.33	21.85	21.70
VectorScal-src	19.61	14.11	4.73	17.45	10.40	21.04	10.49	13.98
TempScal-src	15.12	8.37	4.12	10.86	8.23	13.25	8.07	9.72
CPCS	21.96	14.58	8.22	7.26	7.52	23.23	4.31	12.44
TransCal	6.58	11.28	14.28	10.21	12.67	7.18	13.10	10.76
Ensemble	19.74	16.66	9.08	16.51	12.48	19.31	14.03	15.40
PseudoCal	**3.40**	**4.44**	**1.50**	**2.23**	**0.81**	**2.12**	**1.79**	**2.33**
Oracle	0.86	1.75	1.21	1.11	0.78	0.57	1.06	1.05
Accuracy (%)	48.14	48.65	66.40	50.54	59.89	47.18	56.17	53.85

Table 24: ECE (%) of a closed-set UDA method MCD [6] on *DomainNet*.

Method	C → S	P → C	P → R	R → C	R → P	R → S	S → P	avg
No Calib.	12.97	9.47	3.80	9.65	7.01	12.89	7.80	9.08
MatrixScal-src	31.47	19.56	10.05	20.32	14.30	24.98	18.45	19.88
VectorScal-src	19.63	12.59	5.75	16.53	10.21	20.95	10.27	13.70
TempScal-src	11.61	5.39	4.06	7.58	7.19	10.79	6.74	7.62
CPCS	19.75	6.09	1.96	7.94	3.92	23.82	3.10	9.51
TransCal	19.44	21.53	27.45	21.44	25.19	18.45	24.79	22.61
Ensemble	11.60	7.54	2.86	6.95	5.35	11.07	5.19	7.22
PseudoCal	**1.66**	**3.60**	**1.01**	**0.93**	**1.11**	**1.73**	**1.21**	**1.61**
Oracle	0.62	1.81	0.56	0.85	0.91	0.73	1.03	0.93
Accuracy (%)	49.09	48.21	65.32	49.49	59.58	46.81	56.40	53.56

Table 25: ECE (%) of closed-set UDA methods on *Office-31*.

Method	ATDOC [21]					BNM [32]					MCC [33]				
	A → D	A → W	D → A	W → A	avg	A → D	A → W	D → A	W → A	avg	A → D	A → W	D → A	W → A	avg
No Calib.	4.59	6.66	11.43	12.91	8.90	11.12	8.27	24.60	22.22	16.55	6.18	7.80	18.60	19.97	13.14
MatrixScal-src	9.58	13.21	14.04	15.35	13.05	11.22	8.81	24.64	21.94	16.65	9.70	10.21	18.99	21.84	15.19
VectorScal-src	4.57	6.43	15.69	17.50	11.05	8.15	4.11	24.82	23.59	15.17	5.12	3.16	20.53	24.01	13.21
TempScal-src	**3.39**	4.18	24.37	20.41	13.09	9.23	4.98	26.15	21.55	15.48	3.79	3.00	22.07	20.70	12.39
CPCS	7.98	8.94	26.49	22.80	16.55	11.65	**2.02**	27.16	17.73	14.64	4.69	3.03	29.84	30.47	17.01
TransCal	14.21	14.64	13.27	11.02	13.29	**5.22**	2.70	16.00	13.72	9.41	3.77	3.91	5.57	7.49	5.19
Ensemble	3.60	**4.09**	9.04	10.53	6.82	6.92	4.63	19.99	19.56	12.78	3.07	4.88	17.18	17.78	10.73
PseudoCal	6.64	4.98	**3.22**	**4.47**	**4.83**	6.30	3.97	**10.75**	**8.21**	**7.31**	**2.68**	**2.82**	**4.50**	**4.71**	**3.68**
Oracle	2.49	3.15	1.90	2.35	2.47	2.65	1.40	2.63	2.41	2.27	2.36	2.67	2.42	2.05	2.38
Accuracy (%)	91.57	88.93	73.41	73.06	81.74	88.35	90.94	71.35	73.77	81.10	91.37	89.06	69.86	69.51	79.95

Table 26: ECE (%) of closed-set UDA methods on *Office-31*.

Method	CDAN [5]					SAFN [34]					MCD [6]				
	A → D	A → W	D → A	W → A	avg	A → D	A → W	D → A	W → A	avg	A → D	A → W	D → A	W → A	avg
No Calib.	9.34	7.96	16.66	17.39	12.84	6.17	6.68	20.34	22.33	13.88	9.49	8.88	16.39	17.03	12.95
MatrixScal-src	11.90	14.91	17.21	21.12	16.29	9.49	13.97	20.56	23.43	16.86	9.83	13.49	17.86	20.28	15.37
VectorScal-src	6.04	3.60	17.67	25.37	13.17	3.22	**2.20**	21.07	23.59	12.52	5.87	4.61	17.75	20.52	12.19
TempScal-src	5.70	3.41	16.10	20.97	11.55	3.21	2.83	24.48	23.41	13.48	**3.44**	**2.36**	32.09	18.65	14.14
CPCS	30.95	5.67	**4.99**	29.95	17.89	8.21	18.21	24.18	22.12	18.18	11.85	19.01	32.45	22.92	21.56
TransCal	7.44	6.84	5.51	**4.18**	5.99	**3.04**	2.81	6.43	9.86	5.54	5.65	4.76	5.86	4.39	5.17
Ensemble	4.98	3.29	7.41	14.43	7.53	3.81	5.75	17.58	20.20	11.84	6.25	5.49	13.53	15.60	10.22
PseudoCal	**4.78**	**3.04**	6.39	6.78	**5.25**	7.92	5.51	**4.00**	**4.26**	**5.42**	5.97	5.33	**4.38**	**4.06**	**4.94**
Oracle	3.26	2.17	2.94	3.47	2.96	2.90	1.75	2.14	2.27	2.27	3.55	1.76	2.31	1.90	2.38
Accuracy (%)	87.15	87.17	64.82	67.23	76.59	89.96	88.55	69.33	68.58	79.11	86.14	85.53	67.52	66.63	76.46

Table 27: ECE (%) of a partial-set UDA method ATDOC [21] on *Office-Home*.

Method	Ar → Cl	Ar → Pr	Ar → Re	Cl → Ar	Cl → Pr	Cl → Re	Pr → Ar	Pr → Cl	Pr → Re	Re → Ar	Re → Cl	Re → Pr	avg
No Calib.	28.21	20.87	10.76	17.58	23.49	11.69	19.16	28.98	14.34	13.29	28.22	15.64	19.35
MatrixScal-src	35.85	19.37	13.42	29.69	30.20	21.94	21.96	37.00	14.83	19.36	34.96	16.94	24.63
VectorScal-src	25.87	15.83	7.46	18.37	20.96	11.63	19.96	33.03	12.36	11.16	26.57	11.61	17.90
TempScal-src	21.08	15.04	5.75	12.95	17.86	7.52	18.23	29.63	12.88	9.02	23.66	11.83	15.45
CPCS	28.34	27.40	19.28	14.37	6.27	10.86	32.51	39.04	13.75	11.28	21.84	7.92	19.41
TransCal	**4.36**	**5.07**	10.58	9.47	**4.98**	12.82	**9.12**	**5.81**	10.51	13.32	**5.34**	7.60	8.25
Ensemble	20.32	12.06	8.90	11.80	17.57	7.89	12.32	22.25	9.07	11.81	21.26	10.68	13.83
PseudoCal	9.15	7.08	**3.21**	**7.59**	7.53	**4.84**	11.80	12.79	**6.45**	**4.21**	10.75	**4.10**	**7.46**
Oracle	3.09	4.24	2.82	4.78	4.93	4.48	4.04	5.03	4.94	3.58	5.24	3.95	4.26
Accuracy (%)	51.46	64.99	77.19	61.89	61.34	73.44	59.50	49.01	70.51	67.68	51.64	71.43	63.34

Table 28: ECE (%) of a partial-set UDA method MCC [33] on *Office-Home*.

Method	Ar → Cl	Ar → Pr	Ar → Re	Cl → Ar	Cl → Pr	Cl → Re	Pr → Ar	Pr → Cl	Pr → Re	Re → Ar	Re → Cl	Re → Pr	avg
No Calib.	22.91	11.67	8.45	14.42	14.34	10.29	12.63	21.14	8.22	11.09	22.46	10.63	14.02
MatrixScal-src	35.16	19.13	14.89	29.94	30.26	25.30	24.67	34.81	14.78	18.58	34.09	15.73	24.78
VectorScal-src	19.52	9.73	6.05	12.79	14.23	11.07	16.13	26.53	9.03	9.29	20.18	7.95	13.54
TempScal-src	13.14	**5.37**	**3.05**	5.96	6.62	**4.21**	10.00	20.08	5.79	5.39	14.70	6.12	8.37
CPCS	19.34	10.62	4.00	4.25	**4.14**	12.00	28.24	37.75	16.08	5.70	27.24	12.51	15.16
TransCal	2.74	6.19	5.25	8.09	5.92	8.40	11.03	6.01	7.29	9.20	**4.06**	**4.13**	6.53
Ensemble	18.27	9.86	6.49	9.68	11.37	7.27	8.76	18.05	6.57	9.21	19.31	9.10	11.16
PseudoCal	**2.51**	7.86	4.70	**3.04**	6.70	5.78	**4.20**	**4.01**	**3.96**	**3.99**	4.36	6.23	**4.78**
Oracle	2.29	3.75	2.04	2.67	3.07	3.11	2.69	3.26	1.97	3.06	3.47	2.35	2.81
Accuracy (%)	51.10	74.17	81.56	62.53	66.72	73.16	63.27	50.03	79.96	70.80	53.91	79.33	67.21

Table 29: ECE (%) of a partial-set UDA method PADA [10] on *Office-Home*.

Method	Ar → Cl	Ar → Pr	Ar → Re	Cl → Ar	Cl → Pr	Cl → Re	Pr → Ar	Pr → Cl	Pr → Re	Re → Ar	Re → Cl	Re → Pr	avg
No Calib.	20.35	8.33	5.30	11.10	12.28	10.19	8.93	18.60	4.83	8.31	18.33	6.95	11.13
MatrixScal-src	36.55	24.04	16.23	34.97	33.22	28.87	27.26	37.58	16.54	20.45	35.41	16.45	27.30
VectorScal-src	20.53	7.22	4.71	12.28	13.91	13.44	22.41	31.95	9.35	9.07	19.86	8.57	14.44
TempScal-src	15.15	6.09	3.34	6.51	6.43	**4.64**	13.91	23.77	4.27	6.34	15.69	6.11	9.35
CPCS	24.22	30.26	24.81	9.80	7.37	43.23	28.84	39.45	14.97	34.57	4.55	14.27	23.03
TransCal	9.39	23.43	26.71	21.37	20.51	21.88	22.49	11.25	31.71	24.23	12.37	25.06	20.87
Ensemble	11.42	**4.97**	**2.88**	6.02	**4.54**	4.65	**3.76**	11.15	**4.24**	6.13	13.00	**3.79**	**6.38**
PseudoCal	**2.95**	12.31	7.51	**4.68**	10.14	5.38	5.77	**4.13**	7.19	**3.71**	**3.28**	9.85	6.41
Oracle	2.16	5.65	2.27	3.89	5.70	2.83	5.06	2.73	3.98	2.87	3.06	3.06	3.61
Accuracy (%)	43.82	59.83	72.45	51.70	52.32	58.14	51.52	40.66	69.02	63.73	47.70	71.54	56.87

Table 30: ECE (%) of a white-box source-free UDA method SHOT [11] on *DomainNet*.

Method	C → S	P → C	P → R	R → C	R → P	R → S	S → P	avg
No Calib.	21.57	16.14	10.03	18.18	20.86	24.71	21.52	19.00
MatrixScal-src	27.18	19.67	12.49	19.13	16.99	21.60	20.35	19.63
VectorScal-src	17.79	13.95	6.46	19.31	16.25	22.17	13.20	15.59
TempScal-src	13.91	11.32	4.81	16.76	16.47	18.99	10.63	13.27
CPCS	12.52	7.28	4.93	13.64	10.86	16.57	9.10	10.70
TransCal	16.39	23.80	25.37	24.23	18.18	15.87	14.81	19.81
Ensemble	17.57	13.24	7.81	15.24	18.14	21.40	17.73	15.88
PseudoCal	**5.82**	**6.08**	**2.91**	**7.23**	**7.17**	**7.51**	**8.38**	**6.44**
Oracle	2.03	3.69	1.37	2.85	2.25	2.33	2.78	2.47
Accuracy (%)	59.80	66.79	78.34	66.25	66.08	59.48	62.88	65.66

Table 31: ECE (%) of a black-box source-free UDA method DINE [19] on *DomainNet*.

Method	C → S	P → C	P → R	R → C	R → P	R → S	S → P	avg
No Calib.	31.91	22.54	12.39	21.43	20.63	28.77	24.38	23.15
Ensemble	26.38	18.72	10.83	17.03	17.53	24.28	20.18	19.28
PseudoCal	**17.86**	**15.12**	**5.30**	**13.71**	**11.14**	**14.44**	**14.75**	**13.19**
Oracle	1.35	1.87	1.29	1.62	1.94	1.38	1.65	1.59
Accuracy (%)	54.26	63.00	80.69	64.52	67.13	56.75	63.81	64.31